

PREPARED FOR SUBMISSION TO JHEP

ZU-TH 34/14
MCnet-14-22
LPN14-116
MITP/14-072
CERN-PH-TH-2014-192

Higgs boson pair production in the $D = 6$ extension of the SM

Florian Goertz,^{1,2} Andreas Papaefstathiou,^{2,3} Li Lin Yang,^{4,5,6} José Zurita.⁷¹*Institute for Theoretical Physics, ETH Zürich, CH-8093 Zürich, Switzerland*²*PH Department, TH Unit, CERN, CH-1211 Geneva 23, Switzerland*³*Physik-Institut, Universität Zürich, CH-8057 Zürich, Switzerland*⁴*School of Physics and State Key Laboratory of Nuclear Physics and Technology, Peking University, Beijing 100871, China*⁵*Collaborative Innovation Center of Quantum Matter, Beijing, China*⁶*Center for High Energy Physics, Peking University, Beijing 100871, China*⁷*PRISMA Cluster of Excellence & Mainz Institute for Theoretical Physics Johannes Gutenberg University, 55099 Mainz, Germany**E-mail:* florian.goertz@cern.ch, apapaefs@cern.ch, yanglilin@pku.edu.cn, jose.zurita@uni-mainz.de

ABSTRACT: We derive the constraints that can be imposed on the dimension-6 effective theory extension of the Standard Model, using gluon fusion-initiated Higgs boson pair production at the LHC. We use a realistic analysis focussing on the $hh \rightarrow (b\bar{b})(\tau^+\tau^-)$ final state, including initial-state radiation and non-perturbative effects. We include the statistical uncertainties on the signal rates as well as conservative estimates of the theoretical uncertainties. We first consider a theory containing only modifications of the trilinear coupling, through a $c_6\lambda H^6/v^2$ Lagrangian term, and then examine the full parameter space of the effective theory, incorporating current bounds obtained through single Higgs boson measurements. We also consider an alternative scenario, where we vary a smaller sub-set of parameters. Allowing, finally, the values of the other coefficients to vary within *projected* experimental ranges, we find that the currently unbounded parameter, c_6 , could be constrained to lie within $|c_6| \lesssim 0.6$ at 1σ confidence, at the end of the high-luminosity run of the LHC (14 TeV) in the full model, and to $-0.6 \lesssim c_6 \lesssim 0.5$ in the alternative model. This study constitutes a first step towards the inclusion of multi-Higgs boson production in a full fit to the dimension-6 effective field theory framework.

Contents

1	Introduction	1
2	Higgs boson effective theory	3
3	Gluon fusion-initiated multi-Higgs production	4
3.1	Relevant Lagrangian terms	4
3.2	From SM EFT to dimension-6 EFT	5
4	Higgs boson decays in dimension-6 EFT	8
5	Constraining dimension-6 EFT coefficients	10
5.1	Monte Carlo	10
5.2	Analysis	11
5.3	Results	12
5.3.1	c_6 -only model	12
5.3.2	The full model	15
5.3.3	$c_6 - c_t - c_b - c_\tau$ model	19
5.3.4	Summary of results and projected constraints	20
6	Conclusions	23
7	Acknowledgements	24
A	SM $D = 6$ Lagrangian	24
B	Electroweak symmetry breaking with dimension-6 operators	25

1 Introduction

The scalar particle recently discovered by the ATLAS [1] and CMS [2] collaborations at the Large Hadron Collider (LHC) appears to be compatible with the Higgs boson of the Standard Model (SM) [3–5]. In particular, it seems to behave like a CP-even scalar, with couplings to the gauge bosons and fermions that agree at the $\mathcal{O}(20\text{--}100)\%$ level [6–8] with those predicted by the SM, in the cases where the experiments are already sufficiently sensitive (gauge bosons and third generation fermions). The couplings to the SM fields have been probed via the production and decay modes of the Higgs boson and this is a programme that will continue in future runs of the LHC and forthcoming colliders.

The story is different, however, in the “pure Higgs” sector, characterised by the following ($D \leq 4$) potential post-electroweak symmetry breaking (EWSB):

$$V(h) = \frac{1}{2}m_h^2 h^2 + \lambda v h^3 + \frac{1}{4}\tilde{\lambda}h^4, \quad (1.1)$$

where the self-couplings $\lambda = \tilde{\lambda} = m_h^2/2v^2$ within the SM, with $v \simeq 246$ GeV the vacuum expectation value.¹ Specifically, only the first term of Eq. (1.1) has been probed, through the measurement of the Higgs boson mass, $m_h \simeq 125$ GeV. Hence, direct determination of the terms proportional to h^3 and h^4 is an *essential* experimental measurement that will provide access to new phenomena, such as a richer scalar sector or heavier coloured particles, or (in a rather grim scenario) put the validity of the SM on even more solid grounds.

At colliders, terms proportional to h^n can be probed through the simultaneous production of $(n - 1)$ Higgs bosons.² Unfortunately, the production rates for these processes are not as big as for the single Higgs boson production processes, mainly due to the relatively large invariant mass of the final state system. At the LHC with 14 TeV proton-proton centre-of-mass energy, triple production is expected to be rather rare, with a cross section of $\mathcal{O}(0.1)$ fb. This renders any measurement of the coefficient of the h^4 term hard, if not impossible, even at the high-luminosity LHC (HL-LHC) [10–12]. The prospects for Higgs boson pair production are significantly better, with a SM cross section almost three orders of magnitude larger (about 30–40 fb [13–19]). However, this process is still particularly challenging to detect, both in the SM [20–31] and beyond [9, 12, 32–59]. Moreover, sensitivities to the double Higgs boson production process do not immediately translate to sensitivities to the trilinear coupling. The reason is that several diagrams contribute to the production process, but only few of them involve the parameter λ , that are furthermore associated with an off-shell Higgs propagator.

Since no new particles beyond the SM have been observed by the LHC experiments so far, they are either well hidden, weakly coupled, or simply heavier than a (couple of) TeV. In the latter case one can adopt an effective field theory (EFT) approach, where the effects of the high-scale physics are parametrised by a set of higher-dimensional operators, suppressed by a large mass scale Λ . In the present paper we investigate the Higgs boson pair production (hh) in the framework of the dimension-6 effective field theory (D=6 EFT) extension of the SM, modifying in particular (but not only) the Higgs boson potential (1.1). This allows us to derive model-independent constraints on new physics that may be beyond direct reach. The hh process can be a source of additional meaningful information, cutting through regions of the parameter space of the EFT coefficients in non-trivial ways. For example, it may help clarify whether or not the Higgs boson is really part of an $SU(2)_L$ doublet.³ Studying the hh process is essential to probe the full set of the coefficients in the $D = 6$ EFT extension of the SM. In particular, the coefficient of the $D = 6$ operator $\propto H^6$, currently remains unconstrained by single Higgs boson measurements, but can contribute to the hh process through direct modification of the Higgs boson trilinear self-coupling.

¹Measured, e.g. at low energy via four-fermion interactions.

²Although, indirect constraints through loop effects are conceivable. See, for example, [9].

³One can always consider the case where the Higgs is an $SU(2)_L$ singlet and write down the corresponding EFT (see e.g [32, 45, 60–62]). We will not consider this option here.

This paper is organised as follows: in section 2 we examine the EFT Lagrangian containing a complete set of relevant dimension-6 operators, which will form the basis of our investigation. In section 3 we focus on the terms relevant to gluon fusion-initiated Higgs boson pair production after EWSB and compare them to the SM EFT, *i.e.* the SM with the top quark integrated out. In section 4 we examine the impact of the dimension-6 operators on the decays of the Higgs boson and in section 5 we present our setup for the analysis of the key process $pp \rightarrow hh \rightarrow (b\bar{b})(\tau^+\tau^-)$, that we then employ explicitly as an example of our framework to generate constraints. We conclude in section 6. We provide additional information on our conventions in appendix A. Appendix B provides technical details on the derivation of the Lagrangian after EWSB in the $D = 6$ EFT.

2 Higgs boson effective theory

New Physics associated to a new scale $\Lambda \gg v$ can be described in a model-independent way by augmenting the Lagrangian of the SM with all possible gauge-invariant operators of mass dimension $D > 4$, where the leading effects arise from $D = 6$ operators (neglecting lepton-number violating operators, irrelevant to our study). Working at this level, the extension of the SM that we consider for our analysis of Higgs boson pair production reads

$$\begin{aligned}
\mathcal{L} = & \mathcal{L}_{\text{SM}} + \frac{c_H}{2\Lambda^2}(\partial^\mu |H|^2)^2 - \frac{c_6}{\Lambda^2}\lambda |H|^6 \\
& - \left(\frac{c_t}{\Lambda^2} y_t |H|^2 \bar{Q}_L H^c t_R + \frac{c_b}{\Lambda^2} y_b |H|^2 \bar{Q}_L H b_R + \frac{c_\tau}{\Lambda^2} y_\tau |H|^2 \bar{L}_L H \tau_R + \text{h.c.} \right) \\
& + \frac{\alpha_s c_g}{4\pi\Lambda^2} |H|^2 G_{\mu\nu}^a G_a^{\mu\nu} + \frac{\alpha' c_\gamma}{4\pi\Lambda^2} |H|^2 B_{\mu\nu} B^{\mu\nu} \\
& + \frac{ig c_{HW}}{16\pi^2\Lambda^2} (D^\mu H)^\dagger \sigma_k (D^\nu H) W_{\mu\nu}^k + \frac{ig' c_{HB}}{16\pi^2\Lambda^2} (D^\mu H)^\dagger (D^\nu H) B_{\mu\nu} \\
& + \frac{ig c_W}{2\Lambda^2} (H^\dagger \sigma_k \overleftrightarrow{D}^\mu H) D^\nu W_{\mu\nu}^k + \frac{ig' c_B}{2\Lambda^2} (H^\dagger \overleftrightarrow{D}^\mu H) \partial^\nu B_{\mu\nu} \\
& + \mathcal{L}_{\text{CP}} + \mathcal{L}_{4\text{f}},
\end{aligned} \tag{2.1}$$

where α_s is the strong coupling constant and $\alpha' \equiv g'^2/4\pi$.

The full set of $D = 6$ operators that can be formed out of the SM field content was first obtained in [63] and reduced to a non-redundant minimal set in [64]. Here, we employed equations of motion to move to the basis used in [65, 66] and then imposed constraints from precision tests to neglect a class of operators whose effect is already constrained to be at most 1% with respect to the SM, following [67–71]. Including these operators would have a negligible numerical impact on the analysis, given the experimental and theoretical errors.⁴

Precision measurements also lead to the approximate restrictions [65]

$$\frac{c_{HB}}{16\pi^2} = -\frac{c_{HW}}{16\pi^2} = -c_B = c_W, \tag{2.2}$$

⁴In our numerical study, we also neglect possible small CP-odd effects, described by \mathcal{L}_{CP} , as well as effects from four-fermion operators $\mathcal{L}_{4\text{f}}$, which could enter the relevant background processes at leading order. See appendix A for details. Note that, in order to translate to the form of the basis used in [65, 66], we have assumed a trivial flavour structure for the latter operators. See Ref. [72] for a detailed discussion.

which we will employ in the following. Thus our setup corresponds to a restricted strongly-interacting light Higgs (SILH) Lagrangian [73] where c_T has been set to zero and the relations (2.2) are used. We also assume minimal flavour violation (MFV) [74], which leads to the coefficients of the Yukawa-like terms in the second row of Eq. (2.1) being proportional to the (SM-like) Yukawa couplings $y_{t,b,\tau}$ and in particular allows to neglect the corresponding contributions involving the light fermions, hence $Q_L = (t_L, b_L)$ and $L_L = (\nu_\tau, \tau_L)$. Note that the latter can also be justified without assuming MFV [75]. In particular, this helps to exclude the possibility of largely-modified hierarchies in fermion-Higgs couplings with respect to the SM, which might have also spoiled the hierarchies between the different Higgs boson production mechanisms. In order to further simplify the parameter space, we set $c_\tau = c_b$ in one of the scenarios considered in this paper.⁵ Beyond that, we have normalised the operator coefficients $c_{g,\gamma,HB,HW}$ by a loop suppression factor: in any perturbatively-decoupling renormalizable extension of the SM, these operators can only be generated at the loop level (see [76–78]). Moreover, this is also convenient when comparing the $D = 6$ theory with the top quark EFT, that is, the limit where the top quark is integrated out from the SM, as we will discuss in section 3.

After EWSB, several operators might contribute to the same interaction and field redefinitions need to be introduced in order to obtain canonically normalised kinetic terms. We examine the terms relevant to Higgs physics in the next section.

3 Gluon fusion-initiated multi-Higgs production

3.1 Relevant Lagrangian terms

The dimension-6, CP-even, operators listed in the Lagrangian of Eq. (2.1) that affect the production of multiple Higgs bosons via gluon fusion (at leading order) are:

$$\begin{aligned} \mathcal{L}_{h^n} = & -\mu^2|H|^2 - \lambda|H|^4 - (y_t\bar{Q}_L H^c t_R + y_b\bar{Q}_L H b_R + \text{h.c.}) \\ & + \frac{c_H}{2\Lambda^2}(\partial^\mu|H|^2)^2 - \frac{c_6}{\Lambda^2}\lambda|H|^6 + \frac{\alpha_s c_g}{4\pi\Lambda^2}|H|^2 G_{\mu\nu}^a G_a^{\mu\nu} \\ & - \left(\frac{c_t}{\Lambda^2}y_t|H|^2\bar{Q}_L H^c t_R + \frac{c_b}{\Lambda^2}y_b|H|^2\bar{Q}_L H b_R + \text{h.c.}\right), \end{aligned} \quad (3.1)$$

where in the first line we have included the corresponding SM operators that will receive additional contributions in the effective theory.⁶ We now write

$$H = \exp\left(-i\frac{T\cdot\xi}{v}\right)\frac{1}{\sqrt{2}}\begin{pmatrix} 0 \\ v+h \end{pmatrix}, \quad (3.2)$$

where T represents the 3 generators of $SU(2)_L$, ξ represents the 3 Goldstone degrees of freedom that will be absorbed by the gauge bosons, and h is the physical Higgs boson. To

⁵These coefficients modify the process studied here in a rather similar way.

⁶Note that with a slight abuse of notation here, and in Eq. (2.1), we use λ for the quartic coupling in the SM, while in Eq. (1.1) we use it for a generic trilinear coupling. The former λ will be expressed in terms of v and m_h after minimisation of the Higgs potential. See appendix B for details.

obtain canonical normalisation of the Higgs field, we choose to perform the field redefinition⁷

$$h \rightarrow \left(1 - \frac{c_H v^2}{2\Lambda^2}\right) h - \frac{c_H v}{2\Lambda^2} h^2 - \frac{c_H}{6\Lambda^2} h^3. \quad (3.3)$$

We further redefine $c_i \rightarrow c_i \Lambda^2/v^2$ to absorb the suppression factor into the c_i coefficients. We thus obtain the following interactions in terms of the Higgs boson scalar h , relevant to Higgs boson pair production:

$$\begin{aligned} \mathcal{L}_{hh} = & -\frac{m_h^2}{2v} \left(1 - \frac{3}{2}c_H + c_6\right) h^3 - \frac{m_h^2}{8v^2} \left(1 - \frac{25}{3}c_H + 6c_6\right) h^4 \\ & + \frac{\alpha_s c_g}{4\pi} \left(\frac{h}{v} + \frac{h^2}{2v^2}\right) G_{\mu\nu}^a G_a^{\mu\nu} \\ & - \left[\frac{m_t}{v} \left(1 - \frac{c_H}{2} + c_t\right) \bar{t}_L t_R h + \frac{m_b}{v} \left(1 - \frac{c_H}{2} + c_b\right) \bar{b}_L b_R h + \text{h.c.}\right] \\ & - \left[\frac{m_t}{v^2} \left(\frac{3c_t}{2} - \frac{c_H}{2}\right) \bar{t}_L t_R h^2 + \frac{m_b}{v^2} \left(\frac{3c_b}{2} - \frac{c_H}{2}\right) \bar{b}_L b_R h^2 + \text{h.c.}\right], \end{aligned} \quad (3.4)$$

where we have explicitly written down the contributing components of the Q_L doublets. Naively, all the Wilson coefficients in Eq. (3.1) should be bounded from perturbativity arguments by 4π , and hence if we consider $\Lambda \gtrsim 900$ GeV this automatically implies $|c_i| \lesssim 1$ in Eq. (3.4). For details on the derivation of the terms in the Lagrangian of Eq. (3.4), see appendix B.^{8,9} In Eq. (3.4) we have also given the quartic Higgs self-coupling for completeness. The trilinear and quartic couplings can be written as

$$\begin{aligned} \lambda &= \frac{m_h^2}{2v^2} (1 + \Delta), \\ \tilde{\lambda} &= \frac{m_h^2}{2v^2} \left(1 + 6\Delta + \frac{2}{3}c_H\right), \end{aligned} \quad (3.5)$$

where $\Delta = c_6 - 3c_H/2$. From the above, it can be seen that the SM relation of $\lambda = \tilde{\lambda}$ is broken by the EFT effects: an accurate measurement of both couplings is thus a powerful probe of new physics in the Higgs sector, although, as already mentioned, measurement of the quartic coupling does not seem to be possible in the foreseeable future.

3.2 From SM EFT to dimension-6 EFT

It is useful to compare and contrast the dimension-6 extension of the SM with the EFT that results from taking the top mass to infinity within the SM framework. This will help us in writing down the cross section formula for $gg \rightarrow hh$ in the $D = 6$ EFT.

There are several modifications necessary to incorporate the effect of the $D = 6$ EFT operators in Higgs boson pair production via gluon fusion (see Fig. 1):

⁷This field redefinition [79] involves non-linear terms which remove momentum-dependent Higgs boson interactions that would be less straightforward to implement in a Monte Carlo event generator.

⁸The Feynman rules for the Lagrangian terms appearing in Eq. (3.4) have been checked using the `Mathematica` [80] package `FeynRules` [81, 82].

⁹It is worth stressing here that we expand our couplings around the SM value: in the case of the top-Yukawa the current Higgs boson data possess also a non-SM solution with the *wrong sign* Yukawa. As pointed out in Ref. [83], $gg \rightarrow hh$ could also help to lift the degeneracy, in which case the EFT expansion needs to be performed around the non-SM minima of interest. We do not pursue such an analysis here.

- The Higgs boson self-coupling will be modified according to the first line in Eq. (3.4), represented by modifications of the h^3 vertex in diagram **1A**.
- The top and bottom quark Yukawa couplings will be modified according to the third line in Eq. (3.4). These modifications appear in diagrams **1A** and **1C**.
- The new four-point fermionic interactions $\bar{f}fh^2$ will introduce a new ‘triangle’ diagram, with two Higgs bosons produced at the apex of the triangle. These are described by the fourth line in Eq. (3.4) and appear in diagram **1E**.
- Two new effective theory “tree-level” diagrams will contribute since we now have additional gluon-gluon-Higgs (diagram **1B**) and gluon-gluon-Higgs-Higgs interactions (diagram **1D**), according to the second line in Eq. (3.4).

These are relatively straightforward to incorporate into a Monte Carlo event generator. The shift in the Higgs boson couplings to fermions and to gauge bosons will also lead to changes in its branching ratios. We discuss those changes in section 4.

Our goal is to modify the Standard Model matrix element with finite top mass to readily incorporate the modifications coming from the EFT. We first note that in the heavy top mass limit, the ‘low energy theorem’ states that the interactions of one or two Higgs bosons with two gluons are given by:

$$\mathcal{L}_{\text{SM,EFT}} = (G_{\mu\nu}^a G_a^{\mu\nu}) \frac{\alpha_s}{\pi} \left(\frac{h}{12v} - \frac{h^2}{24v^2} \right). \quad (3.6)$$

It is interesting to point out that the $gghh$ interaction that remains in the heavy top mass approximation corresponds to a spin-0 di-gluon state in $gg \rightarrow hh$, while the spin-2 contributions vanish in this limit. In the effective theory language, the spin-2 contributions correspond to operators of higher dimensionality. The differential partonic cross section for gluon fusion-initiated Higgs boson pair production in the SM, with the full top mass dependence, is given by [16]:

$$\frac{d\hat{\sigma}(gg \rightarrow hh)}{d\hat{t}} = \frac{G_F^2 \alpha_s^2}{256(2\pi)^3} [|C_\Delta F_\Delta + C_\square F_\square|^2 + |C_\square G_\square|^2], \quad (3.7)$$

where, in the SM,

$$C_\Delta = \frac{3m_h^2}{\hat{s} - m_h^2}, \quad C_\square = 1. \quad (3.8)$$

F_Δ , F_\square and G_\square are form factors, given e.g. in Ref. [16], in which G_\square corresponds to a spin-2 contribution, while \hat{s} and \hat{t} are the usual Mandelstam invariants. In the limit of large quark mass in the loop, $m_Q \gg \hat{s}$, the form factors reduce to:

$$\begin{aligned} F_\Delta &= \frac{2}{3} + \mathcal{O}(\hat{s}/m_Q^2), \\ F_\square &= -\frac{2}{3} + \mathcal{O}(\hat{s}/m_Q^2), \\ G_\square &= \mathcal{O}(\hat{s}/m_Q^2). \end{aligned} \quad (3.9)$$

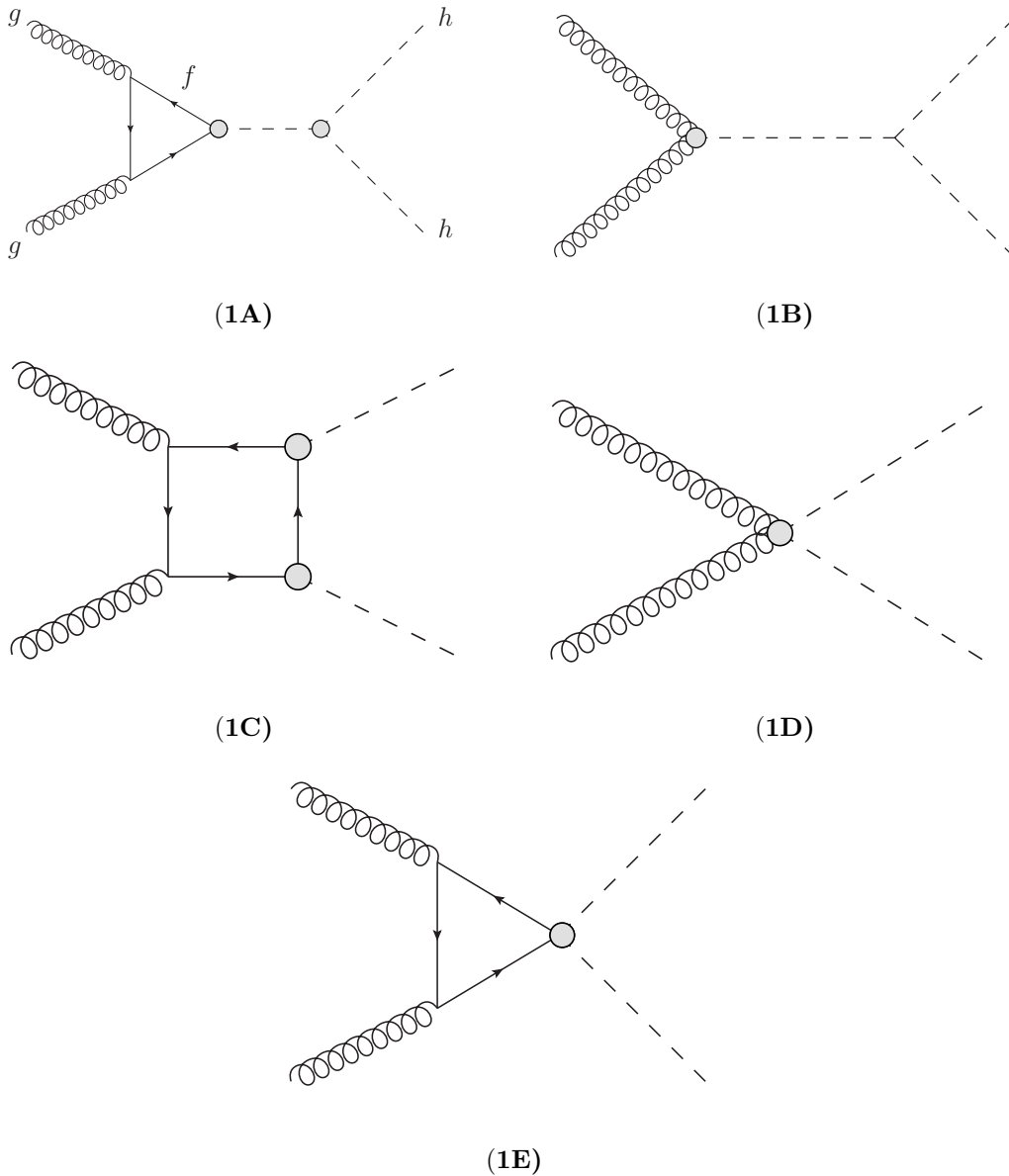


Figure 1: The Feynman diagrams contributing to $gg \rightarrow hh$, including those induced by higher-dimensional operators. The grey blobs indicate the points of insertion of $D = 6$ EFT vertices. At the order that we are considering in the present article, no two EFT insertions can occur in a single diagram. Diagrams with only one grey blob only appear in the effective theory.

Note that the function G_{\square} is sub-dominant in this limit, in correspondence with the fact that the spin-2 terms are absent in Eq. (3.6).

We now derive, starting from Eq. (3.7), the cross section for the hh process in the $D = 6$ EFT. The complete set of diagrams is shown in Fig. 1. Using the above limiting

values of the form factors, one can re-write the Lagrangian of Eq. (3.6) as:

$$\mathcal{L}_{\text{SM,EFT}} = (G_{\mu\nu}^a G_a^{\mu\nu}) \frac{\alpha_s}{8\pi} \left(\frac{h}{v} F_{\Delta}^{\text{hq}} + \frac{h^2}{2v^2} F_{\square}^{\text{hq}} \right), \quad (3.10)$$

where $F_{\Delta}^{\text{hq}} = -F_{\square}^{\text{hq}} = 2/3$ are the values of the form factors in the heavy quark effective theory:

$$F_{\star}^{\text{hq}} = \lim_{m_t \rightarrow \infty} F_{\star}, \quad \star = \{\square, \Delta\}. \quad (3.11)$$

We begin by considering the correspondence between diagrams **1A** and **1B** as well as between **1C** and **1D**. This corresponds to comparing equivalent terms in Eq. (3.10) and Eq. (3.4). We can immediately conclude that the following identifications can be made at the amplitude level to obtain the contributions of the pure EFT diagrams:

$$\begin{aligned} \frac{\alpha_s}{8\pi v} F_{\Delta}^{\text{hq}} &\rightarrow \frac{\alpha_s}{4\pi v} c_g, \\ \frac{\alpha_s}{16\pi v^2} F_{\square}^{\text{hq}} &\rightarrow \frac{\alpha_s}{8\pi v^2} c_g. \end{aligned} \quad (3.12)$$

To obtain diagram **1E**, one needs to essentially ‘remove’ the propagator from a diagram of type **1A**, while keeping the dependence on the quark mass in the triangle loop via the full form factor F_{Δ} . This can be done by multiplying the factor

$$\left[\frac{m_f}{v} \times \frac{3m_h^2}{v} \times \frac{1}{\hat{s} - m_h^2} \right]^{-1} \times 2g_{hhff}, \quad (3.13)$$

which includes a combinatoric factor of 2, $f = t, b$, and

$$g_{hhff} = \frac{m_t}{v^2} \left(\frac{3c_f}{2} - \frac{c_H}{2} \right). \quad (3.14)$$

The necessary additional modifications correspond to trivial replacements of the triple-Higgs coupling and the Yukawa coupling in the SM-like diagrams, according to Eq. (3.4). After all these modifications, we now arrive at the parton-level differential cross section for the process $gg \rightarrow hh$ in the $D = 6$ EFT:

$$\begin{aligned} \frac{d\hat{\sigma}(gg \rightarrow hh)}{d\hat{t}} \Big|_{\text{EFT}} &= \frac{G_F^2 \alpha_s^2}{256(2\pi)^3} \left\{ \left| C_{\Delta} F_{\Delta} (1 - 2c_H + c_t + c_6) + 3F_{\Delta} (3c_t - c_H) + 2c_g C_{\Delta} \right. \right. \\ &\quad \left. \left. + C_{\square} F_{\square} (1 - c_H + 2c_t) + 2c_g C_{\square} \right|^2 + \left| C_{\square} G_{\square} \right|^2 \right\}, \end{aligned} \quad (3.15)$$

where we have suppressed the bottom quark contributions for simplicity.

4 Higgs boson decays in dimension-6 EFT

We now move forward to study the impact of the operators in Eq. (2.1) on the decays of the Higgs bosons. In Table 1 we provide an overview on which coefficients enter the various decays at tree-level topology (second column), at the one-loop level, considering only QCD corrections to the insertions (third column), as well as at the full one-loop level

(fourth column). Here, we focus on the key decays $h \rightarrow bb$, $h \rightarrow \tau\tau$, $h \rightarrow WW$, and $h \rightarrow \gamma\gamma$, that are in particular important for the analysis of Higgs boson pair production. In our numerical study we will, however, consider all significant decays in the EFT. We note that even though operators may not enter a given $pp \rightarrow hh \rightarrow (xx)(yy)$ final state, they will still be relevant since they change the overall branching ratios. We also include in Table 1 the coefficients entering $gg \rightarrow h$ and $gg \rightarrow hh$ production for completeness. It is interesting to observe that several operators may enter both production and decay, introducing non-trivial correlations for the behaviour of the cross section of a given final state mediated through Higgs boson pair production. Finally, note that the presence of the coupling c_γ can lift the $h \rightarrow \gamma\gamma$ decay from one-loop in the SM formally to tree-level in the EFT. The same is true for c_g concerning $gg \rightarrow h$ and $gg \rightarrow hh$. On the other hand, in any perturbatively-decoupling renormalizable extension of the SM the operators c_γ , c_g , c_{HW} and c_{HB} can only be generated at the loop level. Thus, we will in particular not insert them into loop diagrams at the order considered [77].

In the present article we employ the `eHDECAY` code [84] to calculate the branching ratios of the Higgs boson according to our EFT formalism. The program `eHDECAY` provides the SM plus $D = 6$ EFT contributions, including QCD radiative corrections. Next-to-leading order EW corrections are only applied to the SM contributions. For further details, see Ref. [84].

Mode	tree	1 loop QCD	1 loop
$h \rightarrow bb$	$\mathbf{c_H}, \mathbf{c_b}$	$\mathbf{c_H}, \mathbf{c_b}$	c_H, c_b, c_t, c_6, c_W
$h \rightarrow \tau\tau$	$\mathbf{c_H}, \mathbf{c_\tau}$	-	c_H, c_τ, c_6, c_W
$h \rightarrow \gamma\gamma$	$\mathbf{c_\gamma}$	-	$c_H, c_b, c_t, c_\tau, c_W$
$h \rightarrow WW$	$\mathbf{c_H}, \mathbf{c_{HW}}, \mathbf{c_W}$	-	$c_H, c_W, c_b, c_t, c_\tau, c_6$
$gg \rightarrow hh$	$\mathbf{c_g}$	$\mathbf{c_t}, \mathbf{c_b}$	$\mathbf{c_t}, \mathbf{c_b}, \mathbf{c_H}, \mathbf{c_6}$
$gg \rightarrow h$	$\mathbf{c_g}$	$\mathbf{c_t}, \mathbf{c_b}, \mathbf{c_H}$	$\mathbf{c_t}, \mathbf{c_b}, \mathbf{c_H}$

Table 1: Operators that modify the decay modes of the Higgs boson relevant to our analysis, with tree-level topology (second column), at the one-loop level, considering only QCD corrections (third column), as well as at the full one-loop level (fourth column). Note that we neglect one-loop insertions of one-loop operators. For completeness, we also include the operators entering $gg \rightarrow h$ and $gg \rightarrow hh$. The operators that are highlighted in bold text are included in the treatment of the present paper, in the corresponding topology. The dashed line separates decay modes that enter our analysis only indirectly in modifications of the Higgs boson branching ratios as well as via the correlations present in the constraints from single Higgs boson physics.

At this point it is worth discussing the loop-suppressed operators $c_{g,\gamma}$ and $c_{HB,HW}$. While the former two induce corrections on Higgs boson decays that appear in the SM at

the one-loop level, the latter affect the $h \rightarrow WW, ZZ$ decays, which are tree level in the SM. Thus, the naive expectation is that the impact of $c_{HW,HB}$ will be essentially negligible on Higgs boson physics. Moreover, due to Eq. (2.2), the loop-suppression of these coefficients feeds through to c_B, c_W via a single free parameter. We have explicitly verified that an $\mathcal{O}(1)$ change in the $c_{HW,HB,W,B}$ coefficients leads to at most a 4 % variation in the loosely-constrained $h \rightarrow Z\gamma$ decay rate and sub-percent level variations in $h \rightarrow WW, ZZ$. The same exercise with c_γ gives instead a $\mathcal{O}(70\%)$ variation in the $h \rightarrow \gamma\gamma$ branching ratio, which is phenomenologically relevant for the single Higgs boson constraints that we will employ. We thus neglect the effect of the operators $\mathcal{O}_W, \mathcal{O}_B, \mathcal{O}_{HB}$ and \mathcal{O}_{HW} in the rest of this paper, but consider variations of c_γ .

5 Constraining dimension-6 EFT coefficients

5.1 Monte Carlo

We have implemented the Lagrangian terms of Eq. (3.4) in a HERWIG++ model where the SM matrix elements have been taken from the code HPAIR [10, 14, 85]. The Monte Carlo event generator is essential to our analysis. This is because a calculation of the total cross section alone cannot account for the change in distributions of momenta and angles that will substantially change the efficiency of the experimental analysis. Thus, even if we do not use their shapes explicitly in extracting constraints in this article, it is essential to have a reliable description of the underlying distributions. One could employ the Monte Carlo-generated distributions to further improve the bounds [86], keeping in mind the fact that operators will mix due to renormalization group running. See for example, Ref. [87].

The calculation of our study is accurate to LO in QCD, within the framework of the $D = 6$ EFT, including the diagrams of Fig. 1. Full QCD corrections to the diagrams that include top quark loops have not yet been calculated with the dependence on the top quark mass. These are available only in the heavy top mass limit (also known as the ‘low-energy theorem’), which provides an estimate of their magnitude. The QCD corrections to the additional new processes that arise in $D = 6$ EFT consist of Feynman diagrams that are of identical topology to those of SM diagrams within the ‘low-energy theorem’. We thus expect the size of the QCD corrections to be similar in all sub-diagrams contributing to the process, including those that only appear in the $D = 6$ EFT. For the sake of simplicity, we apply a flat overall K -factor of $K = 2$, which would correspond to normalizing our result to the state-of-the-art (NNLO QCD) SM calculation of ~ 40 fb [17]. The choice is conservative, and justified at present by the fact that the low-energy theorem in the SM is estimated to possess $\mathcal{O}(10\%)$ uncertainty [12, 19]. This uncertainty is subsumed in the 30% total theoretical uncertainty that we will assume here (see Section 5.2).¹⁰

We start by investigating the individual effects on the gluon fusion production cross section, varying one coefficient at a time, while setting all others to zero. The result is presented in Fig. 2, for the LHC running at 14 TeV proton-proton centre-of-mass energy, where we

¹⁰Moreover, the NNLO calculation of Ref. [17] is not available at present to use for the given parameters that we employ here (i.e. PDF set and scale choices).

have zoomed-in in the right panel, and shaded the $\pm 10\%$ variation region from the SM value of the cross section. Here and in the remaining article, we employ the MSTW2008nlo_nf4 PDF sets [88].¹¹ One can clearly see how deviations from the SM prediction $c_i = 0$ could lead to substantial changes in the total cross section. Unfortunately, the dependence on c_6 is rather mild, whereas the dependence on c_t and c_g is substantially more pronounced. This tendency will be amplified when realistic analysis cuts are considered (see below). The fact that positive values of c_6 lead to a decreased cross section reflects the negative interference between the triangle and box contributions.

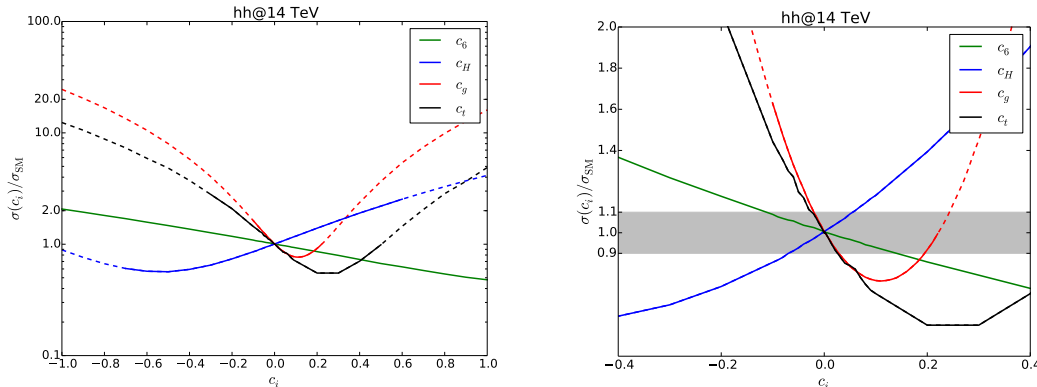


Figure 2: The effect of the variation of individual operators on the total cross section divided by the SM value. In the right panel we focus on a narrower region, showing in the grey-shaded area the $\pm 10\%$ variation with respect to the SM value. The solid portions of the curves represent the region which is compatible at 95% C.L. or more with the current Higgs boson data, obtained using `HiggsBounds` and `HiggsSignals` (see section 5.3.2 for details).

5.2 Analysis

To accommodate a direct comparison with existing phenomenological analyses, we focus on the process $hh \rightarrow (b\bar{b})(\tau^+\tau^-)$ at the 14 TeV LHC. The specific final state possesses a relatively large branching ratio and manageable backgrounds. This channel has been examined in detail within the SM in Refs. [22–24, 29] and turned out to be particularly promising. We consider here only the main irreducible backgrounds, arising from $t\bar{t}$ production with subsequent decays of the W bosons to τ leptons, as well as ZZ and hZ production with $(b\bar{b})(\tau^+\tau^-)$ final states, which is sufficient given the other sources of uncertainty.¹² The backgrounds were generated at next-to-leading order in QCD, using the `aMC@NLO` event generator [89–91]. The total cross section for $t\bar{t}$ was normalised to $\sigma_{t\bar{t}} = 900$ pb [92, 93] and the ZZ and hZ NLO cross sections were taken out of the `aMC@NLO` calculation directly:

¹¹The cross sections have been verified through an independent implementation directly in `HPAIR`.

¹²We have also considered the effect of $D = 6$ operators in hZ production and the subsequent Higgs boson decay. These were found to have negligible impact on our analysis and we do not discuss them in detail.

$\sigma_{ZZ} = 15.25$ pb and $\sigma_{hZ} = 0.8329$ pb. For realistic description of the final states, parton showering and hadronization were performed using `HERWIG++`, and the simulation of the underlying event was included via multiple secondary parton interactions [94].

We follow the basic analysis steps as given originally in [22] and as were described in [29]. Here, we assume 70% τ -reconstruction efficiency with negligible fake rate¹³ and require two τ -tagged jets with at least $p_{\perp} > 20$ GeV. We require that the di-tau invariant mass, taken from the Monte Carlo truth, reproduces the Higgs mass within a ± 25 GeV window, to account for the reconstruction smearing, as done in [22]. To model this effect, we smear the true di-tau invariant mass by a 20 GeV Gaussian, which in turn allows for a contamination from events containing $Z \rightarrow \tau^+ \tau^-$ into the di-tau mass window that we consider. We use the Cambridge-Aachen jet algorithm available in the `FastJet` package [95, 96] with a radius parameter $R = 1.4$ to search for so-called ‘fat jets’. We require the existence of one fat jet in the event satisfying the mass-drop criteria as done in the hV study in Ref. [97]. We require the two hardest ‘filtered’ sub-jets to be b-tagged¹⁴ and to be central ($|\eta| < 2.5$) and the filtered fat jet to be in $(m_h - 25 \text{ GeV}, m_h + 25 \text{ GeV})$, which will reduce events with $Z \rightarrow b\bar{b}$ decays. The b-tagging efficiency was taken to be 70%, again with negligible fake rate for the sake of simplicity. We require a loose cut on the transverse momentum of the fat jet (after filtering) that satisfies the above criteria, $p_{\perp}^{\text{fat}} > 100$ GeV and also apply a transverse momentum cut on the $\tau^+ \tau^-$ system of equal magnitude, $p_{\perp}^{\tau\tau} > 100$ GeV. As in [29], we apply additional cuts: $\Delta R(h, h) > 2.8$ and $p_{\perp}^{hh} < 80$ GeV to reject the background even further.

We investigate the effect of the above analysis on events corresponding to different values of the parameters.¹⁵ On the left panel of Fig. 3 we plot the efficiency of the analysis in the case where we set all other coefficients to zero except the labeled one. On the right panel we show the efficiency times the cross section of the EFT point, divided by the SM cross section ($\sigma_{\text{LO}} = 22.3$ fb) times the SM point efficiency ($\epsilon \simeq 0.065$). This plot can be compared with the actual cross section plot of Fig. 2, where one can observe that the qualitative behaviour of the resulting cross sections does not change, but there is a quantitative change due to the non-uniform effect of the analysis. Note that we have not included the actual branching ratios in Fig. 3, which will have a further effect in determining the significance of a given parameter point.

5.3 Results

5.3.1 c_6 -only model

For simplicity, we begin by considering a model where only c_6 is non-zero and allowed to vary. In fact, this is the only coefficient that remains unconstrained from data on single Higgs boson production. Setting *all* other c_i ’s to zero and varying c_6 corresponds to

¹³Thus, we do not consider any mistagging backgrounds, which should be considered in a full experimental study. These are expected to be sub-dominant, as we require 2 b-tags and 2-tau tags in our analysis.

¹⁴Bottom-jet tagging was performed by setting the bottom mesons to stable in the `HERWIG++` event generator.

¹⁵One could optimize the analysis for each point (or region) in the parameter space. We leave that task for future work [86].

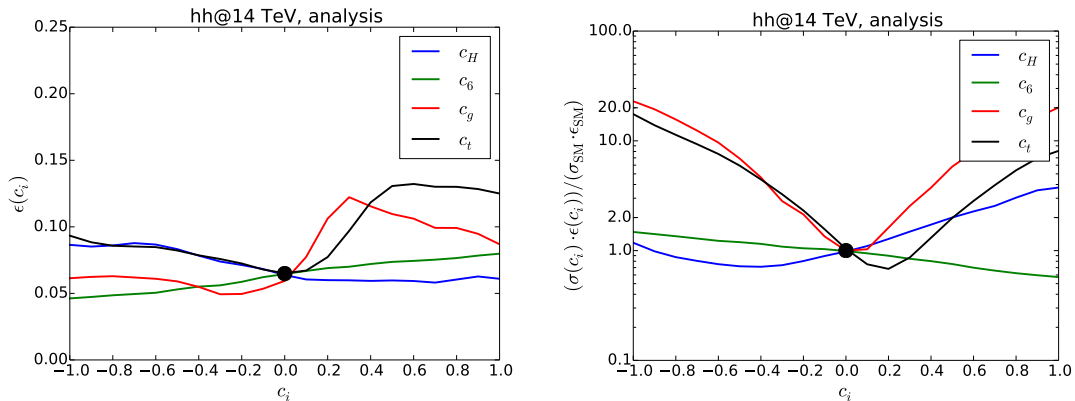


Figure 3: The efficiency of the analysis is shown on the left panel. The right panel shows the efficiency times the cross section of the EFT point, divided by the SM cross section times the SM point efficiency.

modifying the size of the Higgs boson self-coupling λ , as was done in previous studies.¹⁶ The value of c_6 here represents a relative change in λ with respect to the SM prediction. No modifications are expected at the order considered on the Higgs boson decays when including such an operator. We investigate the possible constraints on c_6 given the particular model.¹⁷

Let us assume that in our analysis we obtain $S(c_6)$ events for the signal, for a given value of c_6 , at a given integrated luminosity. For the background, we obtain B events at the same luminosity. Given that the number of events S and B is large enough, we may assume that they are Gaussian-distributed. The total statistical uncertainty on $N(c_6) = S(c_6) + B$ is then given by:

$$\delta N^2 = \delta B^2 + \delta S^2. \quad (5.1)$$

Therefore, if the relative theoretical uncertainty on the cross section prediction is f_{th} , assuming negligible theoretical uncertainty on the background,¹⁸ an addition in quadrature leads to a total uncertainty of:

$$\delta N^2 = \delta B^2 + \delta S^2 + S^2 f_{\text{th}}^2, \quad (5.2)$$

and hence we have that:

$$\delta N^2 = N + S^2 f_{\text{th}}^2. \quad (5.3)$$

¹⁶In particular, in [27] we focused on such a scenario. Moreover, we studied the dependence on the top Yukawa coupling, which (beyond testing consistency with the SM) allows to examine an independent variation of the coefficient of the $\bar{t}_L t_R h$ operator in Eq. (3.4), which is possible in extensions of the SM where the Higgs boson is not part of a $SU(2)_L$ doublet.

¹⁷We note here that negative values of the coefficient c_6 in this model, and in the rest of the paper, should be taken with a grain of salt due to possible effects on vacuum stability. Detailed study of the behaviour of the potential in this regime is left for future work.

¹⁸The assumption is reasonable since the background higher-order calculations exhibit relatively small variations compared to the hh signal. Moreover, the background prediction can be normalised using a signal-free region.

To obtain the expected constraints, we assume that the underlying theory is indeed the SM, which corresponds to $c_6 = 0$ in this scenario. In turn, the expected total number of events is $N(c_6 = 0)$. One then needs to compute how many standard deviations $\delta N(c_6)$ away a given $N(c_6)$, as predicted from theory, is from $N(c_6 = 0)$. This can be translated into a probability (i.e. a p -value) assuming a Gaussian distribution. The results are presented in Fig. 4, for integrated luminosities of 600 fb^{-1} and 3000 fb^{-1} , where we show in the left panel the p -value obtained assuming no theoretical uncertainty and on the right including a theoretical uncertainty of 30%, i.e. $f_{\text{th}} = 0.3$. We choose 30% as a conservative estimate of the uncertainty, incorporating scale ($\mathcal{O}(10\%)$ at NNLO [17]), PDF plus strong coupling constant (also $\mathcal{O}(10\%)$ [17]) as well as heavy top mass approximation uncertainties (another $\mathcal{O}(10\%)$ [19]).

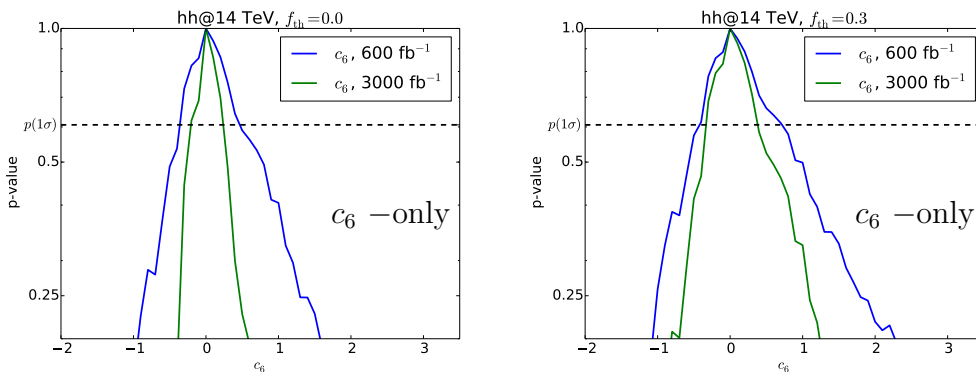


Figure 4: The p -value obtained for a given value of c_6 , for the process $hh \rightarrow (b\bar{b})(\tau^+\tau^-)$ at 600 fb^{-1} and 3000 fb^{-1} of integrated luminosity. On the left figure we show the result without any theoretical uncertainty included ($f_{\text{th}} = 0$) and on the right figure with theoretical uncertainty on the signal cross section prediction of 30% ($f_{\text{th}} = 0.3$).

The values of c_6 compatible with $N(c_6 = 0)$ within 1σ , i.e. the probability drops from $p = 1$ (in our normalization) to $p = \exp(-1/2) \approx 0.607$, and thus the expected constraints, are:

$$\begin{aligned}
 c_6^{1\sigma}(600 \text{ fb}^{-1}) &\in (-0.4, 0.5), & c_6^{1\sigma}(3000 \text{ fb}^{-1}) &\in (-0.3, 0.3), & \text{for } f_{\text{th}} = 0, \\
 c_6^{1\sigma}(600 \text{ fb}^{-1}) &\in (-0.5, 0.8), & c_6^{1\sigma}(3000 \text{ fb}^{-1}) &\in (-0.4, 0.4), & \text{for } f_{\text{th}} = 0.3.
 \end{aligned}
 \tag{5.4}$$

These results are compatible with our previous studies in [27] if the top Yukawa coupling is kept at its SM value. The bounds are weaker for positive c_6 , since this leads to a reduced cross section and thus to a larger statistical uncertainty. The improvement of the 1σ regions is moderate for $f_{\text{th}} = 0.3$ for an increased luminosity, as in that case the uncertainty is dominated by the systematic uncertainty on the theoretical prediction of the signal rates. Improvements on the theoretical description of the process are thus necessary for improving these bounds.

5.3.2 The full model

Generically, one expects several operators to be present. Here we consider the full parameter space, varying the coefficients in Eq. (3.4), as well as c_γ , within the currently allowed regions. We calculate the p -values in a similar fashion as before: we assume that the standard model is true, i.e. $c_i = 0 \forall i$, and compare the number of events after the analysis is performed with those expected from the SM, calculating how ‘far’ they are in terms of the uncertainty δN . We note that, since we are only considering a single observable, the event rate for a particular signal process, we do not expect the constraints on the full parameter space to be strong. The constraints could be improved either by examining other observables in this process, or optimising the analysis for different points in the parameter space. We do not, however, expect significant qualitative changes in our results. To constrain the full parameter space, a combination of all possible production and decay channels (including various single production and double production processes) could be employed. We leave this endeavour to future work. Nevertheless, the main purpose of the study here is to investigate possible correlations among different operators in this process, and show how future measurements of other coefficients will help the determination of the Higgs potential.

To accommodate for the current allowed range on the parameters $c_g, c_t, c_b, c_H, c_\gamma$ we use the codes `HiggsBounds` [98] and `HiggsSignals` [99] on the `eHDECAY` output. We employ the “effective coupling” mode, where one defines

$$g_{hX} = \frac{\Gamma(h \rightarrow X)}{\Gamma(h \rightarrow X)_{\text{SM}}}, \quad (5.5)$$

for the decay of the Higgs into the final state X . In particular, the single Higgs cross section is then scaled using the effective coupling to gluons, g_{hgg} . More explicitly,

$$g_{hgg} = \frac{\Gamma(h \rightarrow gg)}{\Gamma(h \rightarrow gg)_{\text{SM}}} = \frac{\sigma(gg \rightarrow h)}{\sigma(gg \rightarrow h)_{\text{SM}}}. \quad (5.6)$$

For further details we refer the reader to the `HiggsBounds` manual [98]. We perform our numerical scan as follows. We scan each direction of the (5+1)-dimensional parameter space, covering all coefficients, besides c_6 , in the range $\{-0.5, 0.5\}$ in steps of 0.1, while the latter is allowed to vary in a larger range, $\{-2, 3.5\}$, in steps of 0.5.¹⁹ In this scenario, we assume the coefficients c_b and c_τ to be equal. We feed these coefficients into `eHDECAY` to compute the branching ratios of various decay modes of the Higgs boson. In this step, it is possible that some branching ratios in the output of `eHDECAY` become negative for certain values of the coefficients. This is usually due to destructive interference between the EFT contributions to the decay amplitudes and the SM ones, and we discard these points in our scan.²⁰ These coefficients and branching ratios are then given as input to `HiggsBounds`,

¹⁹We note here the possibility of small cut-off effects in the marginalization procedure due to the choices of these ranges.

²⁰Note that this does not necessarily imply that these parameter points are unphysical, or that the power expansion breaks down at these points. It could be that the SM amplitudes are accidentally suppressed (e.g., loop-suppression for $h \rightarrow \gamma\gamma, gg, Z\gamma$) such that they have similar sizes as the EFT amplitudes. To compute the partial widths in these cases, one should include the square of the EFT amplitudes, even though they are formally of higher order in the power expansion. This feature is not implemented in `eHDECAY`.

which checks if a point is excluded at the 95% C.L. by collider data (LEP, Tevatron and LHC). This step is numerically fast, and allows to easily discard points where the EFT effects would have generated an excess of events in single Higgs boson studies at the 7 or 8 TeV LHC. The surviving points are fed into `HiggsSignals`, which performs a multi-dimensional fit to the Higgs observables and outputs a p -value for each point. We discard points which would have given a substantial deficit (or excess) of events in current Higgs data, and thus we keep only points at the 95% C.L., that is, where the p -value corresponds to less than 2 standard deviations from the mean of a Gaussian distribution.

We now proceed to derive the constraint from hh production onto the parameter space allowed by current experiments. To visualize the constraints in the multi-dimensional parameter space, we will therefore project them onto two-dimensional planes. The parameter c_6 still plays a somewhat distinct role, as it is currently essentially unconstrained, and the information on it will come primarily from multi-Higgs boson production. Thus, all two-dimensional exclusion planes include this parameter. To calculate the allowed two-dimensional regions, we need to marginalize over the remaining dimensions. To accomplish this, for a given point in the (c_i, c_6) -plane, we sum over the p -values obtained by varying along the other dimensions. The final p -value in the 2-D plane then reads

$$p(c_i, c_6) = \frac{\sum_{\{c_f\}} p(c_6, c_i, \{c_f\}) \times p_{\text{HS}}(c_i, \{c_f\})}{\sum_{\{c_f\}} p_{\text{HS}}(c_i, \{c_f\})}, \quad (5.7)$$

where $p_{\text{HS}}(c_i, \{c_f\})$ is the probability assigned to the given point from the `HiggsSignals` code. Dividing out by the sum $\sum_{\{c_f\}} p_{\text{HS}}(c_i, \{c_f\})$ removes the constraints arising due to single Higgs boson data coming from `HiggsSignals` on the given (c_i, c_6) -plane, while taking into account this knowledge in the marginalization over the irrelevant coefficients. Essentially, what one achieves by this normalization, is to have a flat probability distribution on the (c_i, c_6) -plane, *before* any hh data is taken into account.

To account for a proper normalization we divide by the maximum corresponding probability, for the coefficients under consideration:

$$\bar{p}(c_i, c_6) = \frac{1}{\max p(c_i, c_6)} p(c_i, c_6). \quad (5.8)$$

The 1σ -equivalent contours are thus drawn by finding the iso-curve corresponding to $\bar{p}(c_i, c_6) = \exp(-1/2) \approx 0.607$. To obtain a constraint on a single coefficient c_i , we marginalize over all the other coefficients c_j ($j \neq i$). This is done in the same way as prescribed by Eqs. (5.7) and (5.8) given above.

We first consider the (c_H, c_6) -plane in Fig. 5. The coefficient c_H enters all EFT diagrams by changing the Higgs boson wave function in a universal way, and competes with c_6 by reducing the self-coupling contribution in our convention. Since c_H also affects single Higgs boson production, it is already constrained by current experimental data. One sees from Fig. 3 that the production rate after cuts depends mildly on c_H , and therefore no significant improvement on its bound from hh production is expected. Indeed, this fact is evident in Fig. 5, where it is also clear that future knowledge about c_H will not help us to constrain

c_6 very much.²¹ When examining Fig. 5, one should also recall that a change in c_H affects the preferred values of other coefficients due to single Higgs boson constraint, entering the marginalization procedure. We find that, after marginalization over the other coefficients, c_H is constrained to lie in $c_H < 0.4$ according to our 1σ -equivalent definition, at 3000 fb^{-1} and for $f_{\text{th}} = 0.3$.

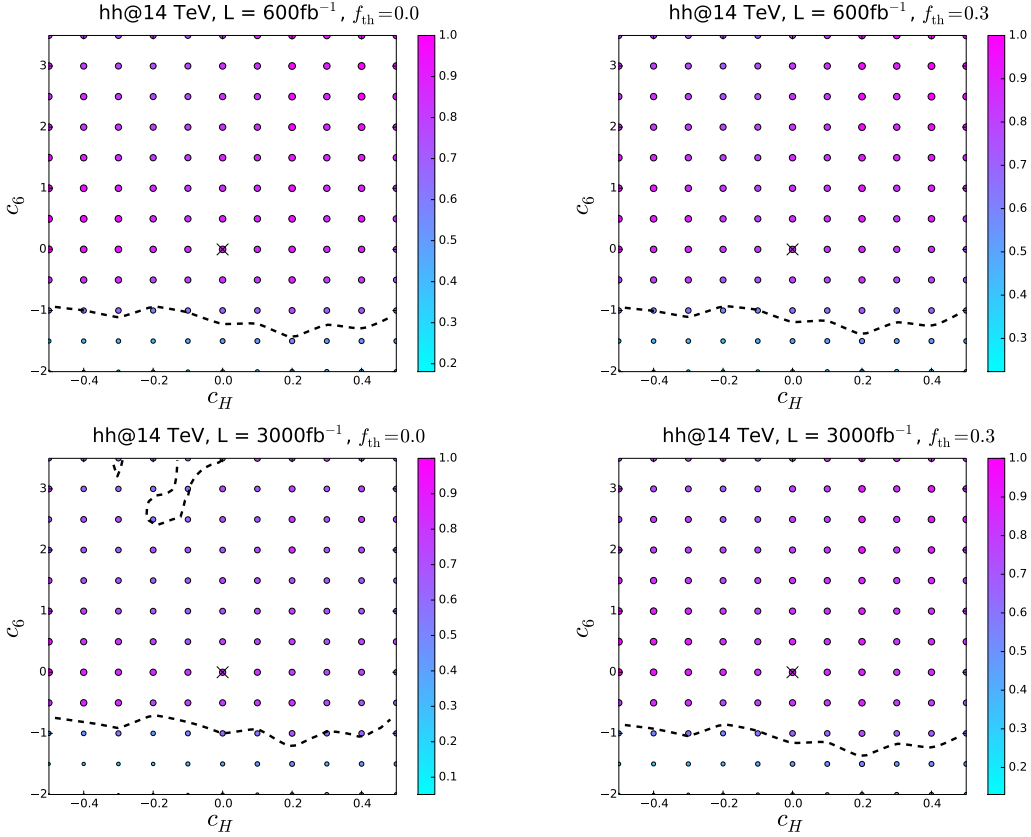


Figure 5: The p -values obtained after marginalization over the directions orthogonal to the (c_H, c_6) -plane, for the process $hh \rightarrow (b\bar{b})(\tau^+\tau^-)$. On the top plots we show the results at 600 fb^{-1} of integrated luminosity, without ($f_{\text{th}} = 0.0$) and with ($f_{\text{th}} = 0.3$) theoretical uncertainty included and on the bottom we show the corresponding plots at 3000 fb^{-1} . We also present the 1-sigma contours as black dashed lines.

We next examine the (c_t, c_6) -plane in Fig. 6. The coefficient c_t enters all diagrams that contain top quarks. Points with positive c_6 and negative c_t are more challenging to exclude – the coefficients enter in the first line of Eq. (3.15) with the same sign, which leads to a compensation of effects (see also Fig. 3). The ‘dip’ structure that appears at $c_t \approx 0.1–0.2$ is related to the fact that the minimum cross section as a function of c_t appears in that region. Beyond the dip, the (most important) corrections from the new triangle diagram mediated by the $t\bar{t}hh$ vertex dominate the behaviour of the cross section, while before the dip their

²¹However, improvements of single Higgs boson constraints on the other coefficients will allow for tighter constraints on this plane.

destructive interference with the box contributions leads to a reduction in the cross section. The coefficient is constrained to lie within $-0.1 \lesssim c_t \lesssim 0.4$ at 3000 fb^{-1} and for $f_{\text{th}} = 0.3$, after marginalization (1σ -equivalent). It is evident that improving the knowledge on the poorly-constrained ‘top Yukawa’ c_t , entering hh production in various ways, will be helpful to improve the exclusion range for c_6 .

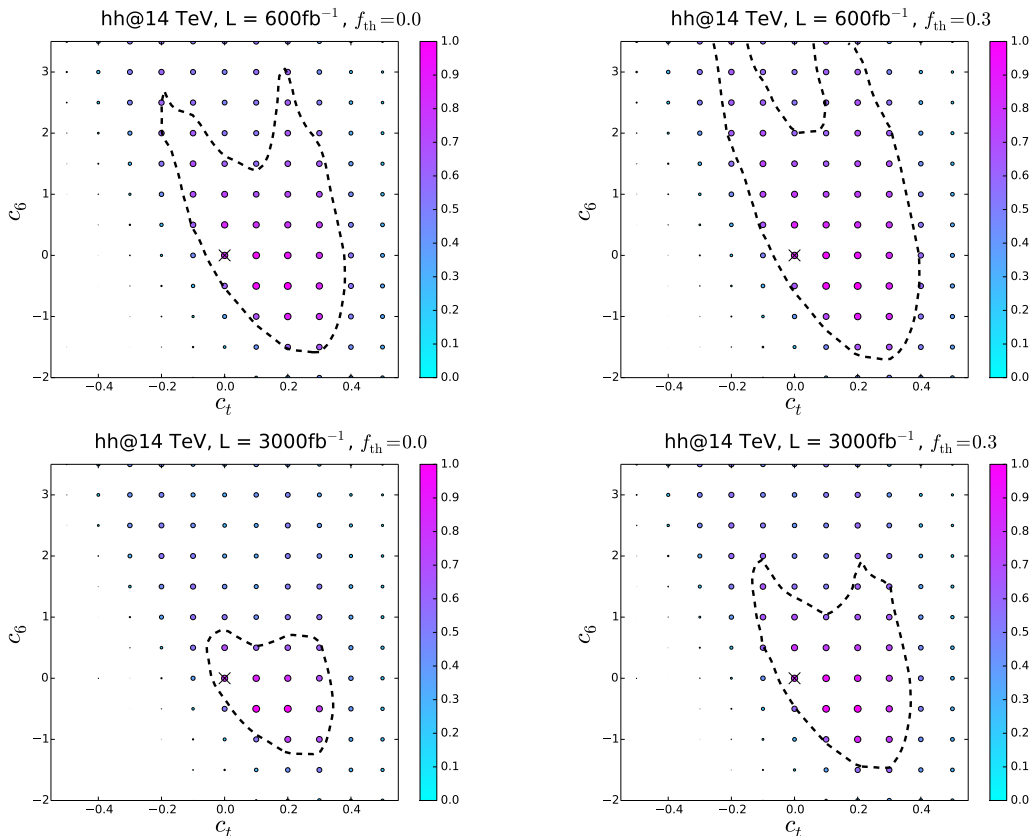


Figure 6: The p -values obtained after marginalization over the directions orthogonal to the (c_t, c_6) -plane, for the process $hh \rightarrow (b\bar{b})(\tau^+\tau^-)$. On the top plots we show the results at 600 fb^{-1} of integrated luminosity, without ($f_{\text{th}} = 0.0$) and with ($f_{\text{th}} = 0.3$) theoretical uncertainty included and on the bottom we show the corresponding plots at 3000 fb^{-1} . We also present the 1 -sigma contours as black dashed lines.

The expected constraints for c_g , which adds tree-level couplings of one or two Higgs boson to two gluons, are shown in the (c_g, c_6) -plane in Fig. 7. The results reflect the fact that an enhanced production cross section due to values of c_g away from the minimum (right panel, Fig. 3) can compensate a reduction due to positive c_6 . The constraint on c_g is found to be $-0.2 \lesssim c_g \lesssim 0.1$ at 3000 fb^{-1} given that $f_{\text{th}} = 0.3$, after marginalization.

We present the results involving c_γ in Fig. 8, which enters the process under consideration indirectly, through modification of the branching ratios (via single Higgs boson data p -values). The correlation with c_6 is weak, and no significant constraint is expected to be imposed through $hh \rightarrow (b\bar{b})(\tau^+\tau^-)$.

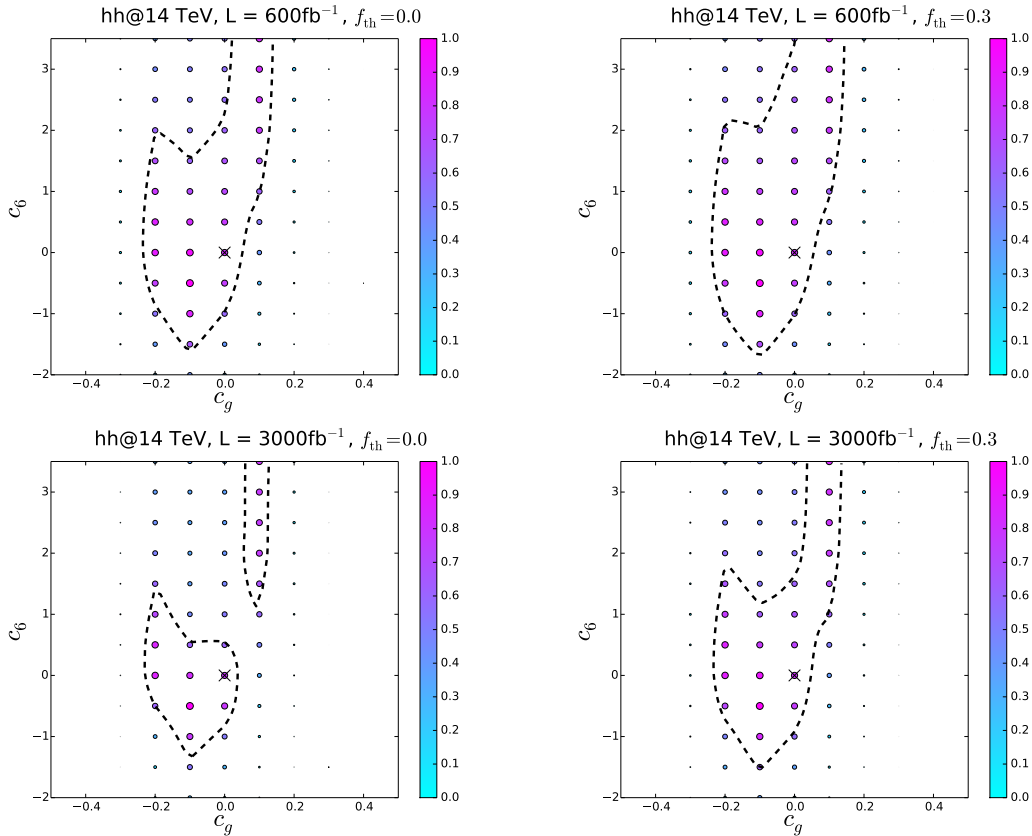


Figure 7: The p -values obtained after marginalization over the directions orthogonal to the (c_g, c_6) -plane, for the process $hh \rightarrow (b\bar{b})(\tau^+\tau^-)$. On the top plots we show the results at 600 fb^{-1} of integrated luminosity, without ($f_{\text{th}} = 0.0$) and with ($f_{\text{th}} = 0.3$) theoretical uncertainty included and on the bottom we show the corresponding plots at 3000 fb^{-1} . We also present the 1-sigma contours as black dashed lines.

The $c_b (= c_\tau)$ coefficient is considered in Fig. 9 on the (c_b, c_6) -plane. Its effects are expected to be sub-dominant in the production due to the assumption of MFV, but it affects the decays of the Higgs boson to $b\bar{b}$ (and $\tau\bar{\tau}$), and hence it is relevant to the process we are considering. The correlation visible reflects the fact that a reduced branching ratio can be compensated by an enhanced production cross section due to a negative value of c_6 . For the given luminosity and $f_{\text{th}} = 0.3$, the resulting bound after marginalization is $-0.2 \lesssim c_b \lesssim 0.3$ at 1σ -equivalent.

Finally, we show the resulting p -values for the coefficient c_6 in Fig. 10 after marginalizing over all the other coefficients. The constraints on c_6 are summarized in detail in Table 3.

5.3.3 $c_6 - c_t - c_b - c_\tau$ model

As a further example, we constrain the non-zero coefficients to be c_6, c_t, c_b and c_τ , varied in the same regions as in the full model. We emphasise that in this scenario, c_τ is allowed to vary independently of c_b . This model includes variations of the coefficients that are

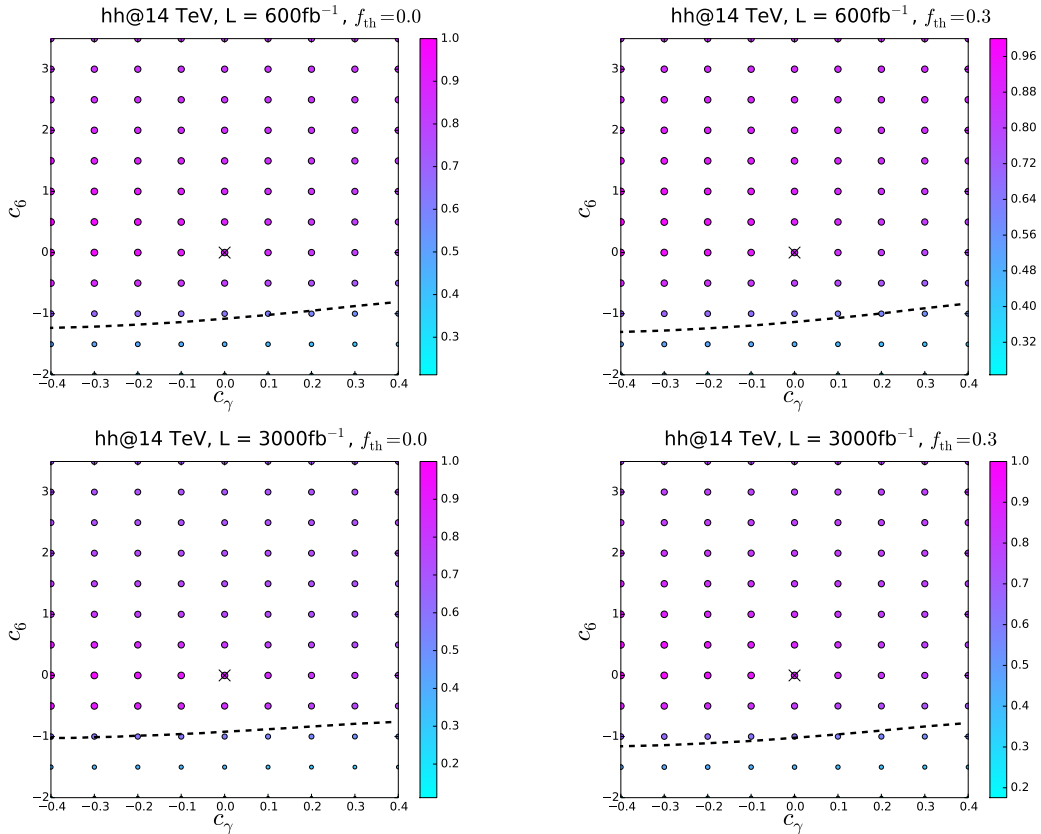


Figure 8: The p -values obtained after marginalization over the directions orthogonal to the (c_γ, c_6) -plane, for the process $hh \rightarrow (b\bar{b})(\tau^+\tau^-)$. On the top plots we show the results at 600 fb^{-1} of integrated luminosity, without ($f_{\text{th}} = 0.0$) and with ($f_{\text{th}} = 0.3$) theoretical uncertainty included and on the bottom we show the corresponding plots at 3000 fb^{-1} . We also present the 1-sigma contours as black dashed lines.

expected to be least constrained by single Higgs experimental data in future runs of the LHC. As in the previous sub-section, we marginalize over all coefficients to obtain bounds on c_6 . The resulting c_6 p -values are shown in Fig. 11 and the summary of results in Table 3.

5.3.4 Summary of results and projected constraints

We now discuss the constraints on c_6 obtained in all cases we considered as shown in Table 3. As explained before, the values take into account the current uncertainty due to the other weakly-bounded coefficients. As expected, the full model, including the current bounds coming from single Higgs boson measurements, provides a wide range for c_6 , at 3000 fb^{-1} ($c_6 \gtrsim -1.2$), when $f_{\text{th}} = 0.3$, whereas the c_6 -only model provides, as expected, a narrower range: $|c_6| \lesssim 0.4$ at 1σ at 3000 fb^{-1} . As an alternative to the full model, our $c_6 - c_t - c_b - c_\tau$ model aims to investigate a smaller set of coefficients, allowing, on the other hand, c_τ to vary as well. The 1σ range in that case is $-1.8 \lesssim c_6 \lesssim 2.3$ at 3000 fb^{-1} .

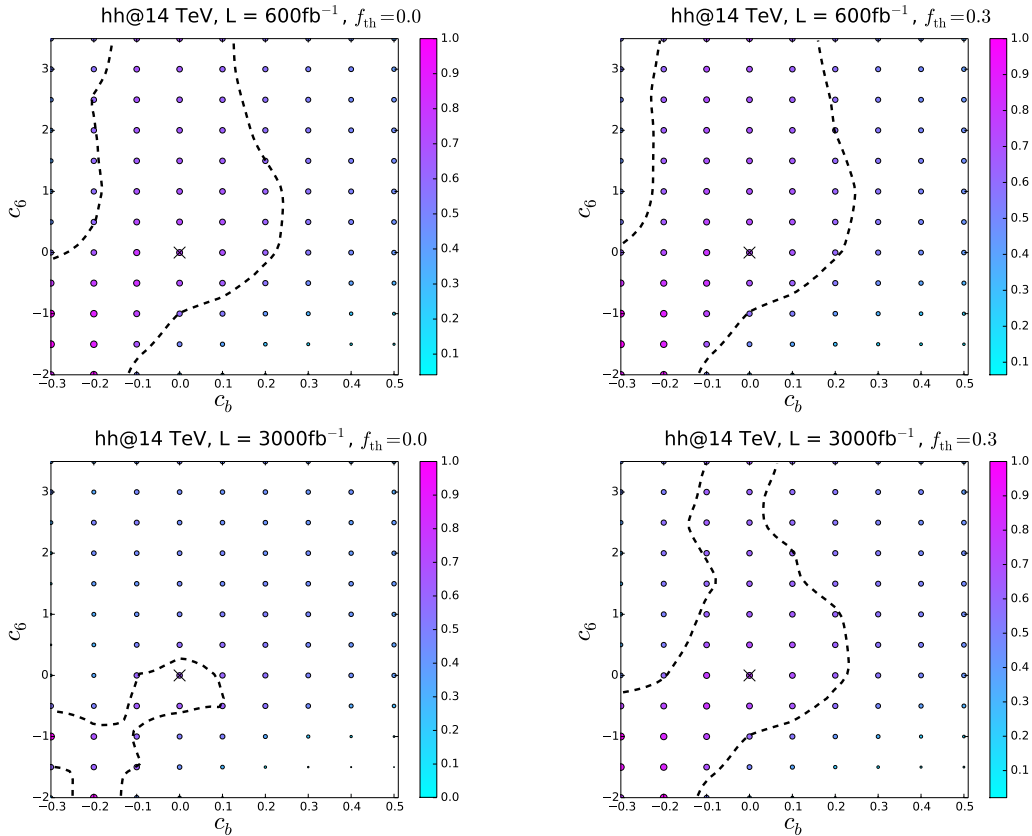


Figure 9: The p -values obtained after marginalization over the directions orthogonal to the (c_b, c_6) -plane, for the process $hh \rightarrow (b\bar{b})(\tau^+\tau^-)$. On the top plots we show the results at 600 fb^{-1} of integrated luminosity, without ($f_{\text{th}} = 0.0$) and with ($f_{\text{th}} = 0.3$) theoretical uncertainty included and on the bottom we show the corresponding plots at 3000 fb^{-1} . We also present the 1-sigma contours as black dashed lines.

Evidently, by the end of the lifetime of the next LHC run (600 fb^{-1}) and the future high-luminosity run (3000 fb^{-1}), the constraints on several of the Wilson coefficients, $c_i (\neq c_6)$ will be substantially improved. The observables used to extract these constraints are complicated functions of these Wilson coefficients. Since it is beyond the scope of this article to predict the shape of the distributions of p -values of the c_f coefficients from these observables, we will assume that these are Gaussian, peaking at the SM value, $\mu_f = 0.0$ with standard deviation Δc_f . The values of Δc_f are calculated in such a way that the effect of coefficients on observables, such as $BR(h \rightarrow \gamma\gamma)$, $BR(h \rightarrow \tau^+\tau^-)$, $BR(h \rightarrow b\bar{b})$ and $\sigma(gg \rightarrow h)$ is $\mathcal{O}(10\%)$. We assume measurement of these quantities to be dominated by systematics at a luminosity of 600 fb^{-1} and hence assume no improvement when going to 3000 fb^{-1} , at the end of the HL-LHC lifetime. The values of Δc_f are summarized in Table 2.

We can then perform the marginalization procedure in a similar manner as prescribed

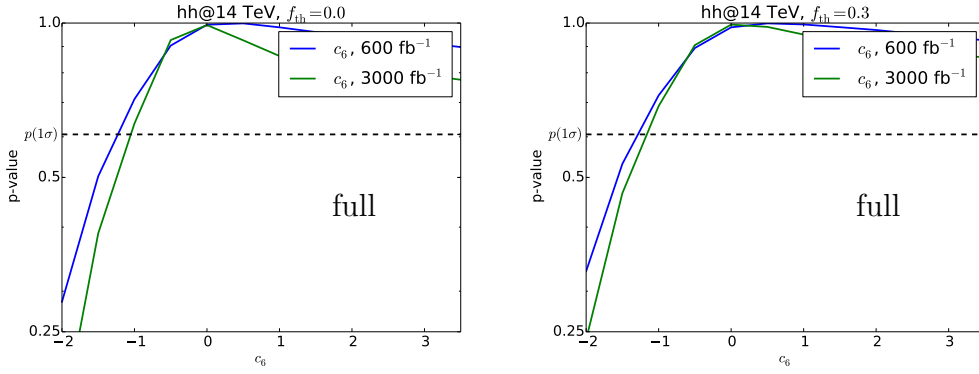


Figure 10: The p -values obtained after marginalization over all coefficients except c_6 in the full model, for the process $hh \rightarrow (b\bar{b})(\tau^+\tau^-)$ at 600 fb^{-1} and 3000 fb^{-1} of integrated luminosity. On the left we show the resulting curves without theoretical uncertainty ($f_{\text{th}} = 0.0$) and on the right we show results with theoretical uncertainty 30% ($f_{\text{th}} = 0.3$).

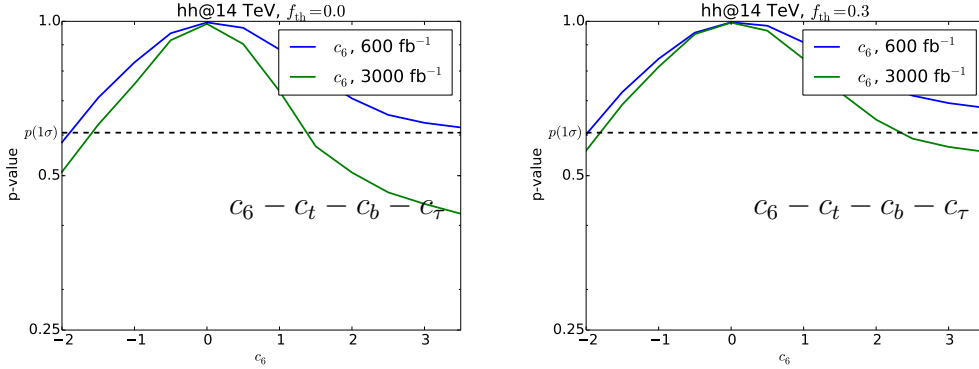


Figure 11: The p -values obtained for c_6 in the $c_6 - c_t - c_b - c_\tau$ model after marginalization, for the process $hh \rightarrow (b\bar{b})(\tau^+\tau^-)$ at 600 fb^{-1} and 3000 fb^{-1} of integrated luminosity. On the left we show the resulting curves without theoretical uncertainty ($f_{\text{th}} = 0.0$) and on the right we show results with theoretical uncertainty 30% ($f_{\text{th}} = 0.3$).

above:

$$p(c_i, c_6) = \frac{\sum_{\{c_f\}} p(c_6, c_i, \{c_f\}) \times p_{\text{Gauss.}}(\{c_f\})}{\sum_{\{c_f\}} p_{\text{Gauss.}}(\{c_f\})}, \quad (5.9)$$

where

$$p_{\text{Gauss.}}(\{c_f\}) = \prod_f \frac{1}{\Delta c_f \sqrt{2\pi}} \exp \left\{ -\frac{(c_f - \mu_f)^2}{2\Delta c_f^2} \right\}. \quad (5.10)$$

After normalization according to Eq. (5.8), this provides an estimate of what constraints would be achievable by combining future single Higgs boson data with the $hh \rightarrow (b\bar{b})(\tau^+\tau^-)$ channel.

Table 3 includes the estimates for the ‘future’ combination, labelled accordingly. We obtain tighter constraints: $|c_6| \lesssim 0.6$ for the full model and $-0.6 \lesssim c_6 \lesssim 0.5$ for the

c_f	Δc_f
c_g	$0.05 \times \frac{1}{3}$
c_H	0.05×2
c_t, c_b, c_τ	0.05
c_γ	$0.05 \times \frac{47}{18}$

Table 2: A summary of the Gaussian errors Δc_f assumed to generate the ‘future’ results at $600 \text{ fb}^{-1}/3000 \text{ fb}^{-1}$ of luminosity of the LHC at 14 TeV. The values are chosen so as to cause $\mathcal{O}(10\%)$ effects on single Higgs boson observables. The numerical factors stem from the normalization with respect to the corresponding SM effect. See, for example, [100].

alternative model at 3000 fb^{-1} , for 30% theoretical uncertainty. Evidently, as expected, these approach the constraints given in the c_6 -only model.

model	$L = 600 \text{ fb}^{-1}$	$L = 3000 \text{ fb}^{-1}$
c_6 -only	$c_6 \in (-0.5, 0.8)$	$c_6 \in (-0.4, 0.4)$
full	$c_6 \gtrsim -1.3$	$c_6 \gtrsim -1.2$
$c_6 - c_t - c_\tau - c_b$	$c_6 \gtrsim -2.0$	$c_6 \in (-1.8, 2.3)$
full (future)	$c_6 \in (-0.8, 0.9)$	$c_6 \in (-0.6, 0.6)$
$c_6 - c_t - c_\tau - c_b$ (future)	$c_6 \in (-0.8, 0.8)$	$c_6 \in (-0.6, 0.5)$

Table 3: A summary of the constraints obtained on the coefficient c_6 at 1σ , at integrated luminosities of 600 fb^{-1} and 3000 fb^{-1} at a 14 TeV LHC, assuming that the theoretical uncertainty on the signal rates is 30%.

6 Conclusions

We have investigated the dimension-6 effective theory description of beyond-the-Standard Model modifications to Higgs boson pair production. Using an implementation within the HERWIG++ Monte Carlo event generator and a realistic analysis, including the description of theoretical uncertainty on the signal rates, we have constructed the possible exclusion regions in a c_6 -only model, a general EFT with all coefficients allowed to vary, and a constrained EFT, marginalising over various parameters in the latter two cases. We find that at the Large Hadron Collider at 14 TeV, meaningful constraints can be obtained on the parameter space of the EFT, particularly on the c_6 coefficient. These results appear in Table 3. We conclude that, approximately, the hitherto unconstrained c_6 would be limited

to $c_6 \gtrsim -1.2$ at 1σ , in the ‘full’ model, given the current constraints on the other coefficients originating from single Higgs boson data, for 3000 fb^{-1} , assuming 30% theoretical uncertainty on the signal rate. In the ‘alternative’ $c_6 - c_t - c_b - c_\tau$ model, this was found to be $-1.8 \lesssim c_6 \lesssim 2.3$. We also provide an estimate of future single Higgs bounds on the Wilson coefficients, by marginalizing over the irrelevant coefficients with a Gaussian probability centred around the SM value ($c_i = 0.0$) with uncertainties that would give $\mathcal{O}(10\%)$ deviations in single Higgs boson observables. This gives tighter constraints for c_6 in the two models: $-0.6 \lesssim c_6 \lesssim 0.6$ for the ‘full’ model and $-0.6 \lesssim c_6 \lesssim 0.5$ for the alternative model at 3000 fb^{-1} , for 30% theoretical uncertainty.

It is clear that the expected bounds could be substantially enhanced, for example, by examining other final states originating from hh , improving the experimental analyses by examining differential distributions and future improvements of the theoretical description of the signal process. Without doubt, our results demonstrate that the process of Higgs boson pair production should be seriously considered as part of the wider programme of constraining the higher-dimensional effective field theory parameter space.

7 Acknowledgements

We would like to thank Brando Bellazzini, Adrian Carmona, Gino Isidori, Zoltan Kunszt, Matthias Neubert, Pedro Schwaller and Luca Vecchi for useful discussions. The research of JZ is supported by the ERC Advanced Grant EFT4LHC of the European Research Council, the Cluster of Excellence Precision Physics, Fundamental Interactions and Structure of Matter (PRISMA-EXC 1098). AP acknowledges support in part by the Swiss National Science Foundation (SNF) under contract 200020-149517, by the European Commission through the ‘‘LHCPhenoNet’’ Initial Training Network PITN-GA-2010-264564, MCnetITN FP7 Marie Curie Initial Training Network PITN-GA-2012-315877 and by a Marie Curie Intra European Fellowship within the 7th European Community Framework Programme (grant no. PIEF-GA-2013-622071). The research of FG has been supported by the Swiss National Foundation under contract SNF 200021-143781 and by a Marie Curie Intra European Fellowship within the 7th European Community Framework Programme (grant no. PIEF-GA-2013-628224).

A SM $D = 6$ Lagrangian

In this section we give more details on the Lagrangian terms not explicitly shown in Eq. (2.1). The part of the SM Lagrangian relevant to our study is given by

$$\mathcal{L}_{SM} = -\mu^2 |H|^2 - \lambda |H|^4 - y_t \bar{Q}_L H^c t_R - y_b \bar{Q}_L H b_R - y_\tau \bar{Q}_L H \tau_R + \text{h.c.} , \quad (\text{A.1})$$

where for simplicity we have only written the Higgs boson couplings to the 3rd generation.

The CP-odd effects are given by

$$\begin{aligned} \mathcal{L}_{CP} = & \frac{\alpha_s \tilde{c}_g}{4\pi \Lambda^2} |H|^2 G_{\mu\nu}^a \tilde{G}_a^{\mu\nu} + \frac{\alpha' \tilde{c}_\gamma}{4\pi \Lambda^2} |H|^2 B_{\mu\nu} \tilde{B}^{\mu\nu} \\ & + \frac{ig \tilde{c}_{HW}}{\Lambda^2} (D^\mu H)^\dagger \sigma_k (D^\nu H) \tilde{W}_{\mu\nu}^k + \frac{ig' \tilde{c}_{HB}}{\Lambda^2} (D^\mu H)^\dagger (D^\nu H) \tilde{B}_{\mu\nu} . \end{aligned} \quad (\text{A.2})$$

In this work we have neglected CP-odd effects for simplicity – these are not expected to contribute to the inclusive cross section at the order considered. Moreover, using current Higgs boson data one can already set some constraints on a Higgs CP-odd component (see e.g. [101–103] and references therein).

Finally, the four-fermion operators, employing the same basis as used in [65], read

$$\begin{aligned}
\mathcal{L}_{4f} = & c_{LR}^t (\bar{Q}_L \gamma^\mu Q_L) (\bar{t}_R \gamma_\mu t_R) + c_{LR}^{(8)t} (\bar{Q}_L \gamma^\mu T^A Q_L) (\bar{t}_R \gamma_\mu T^A t_R) + c_{RR}^t (\bar{t}_R \gamma^\mu t_R) (\bar{t}_R \gamma_\mu t_R) \\
& + c_{LL}^q (\bar{Q}_L \gamma^\mu Q_L) (\bar{Q}_L \gamma_\mu Q_L) + c_{LL}^{(8)q} (\bar{Q}_L \gamma^\mu T^A Q_L) (\bar{Q}_L \gamma_\mu T^A Q_L) \\
& + c_{LR}^l (\bar{L}_L \gamma^\mu L_L) (\bar{\tau}_R \gamma_\mu \tau_R) + c_{RR}^l (\bar{\tau}_R \gamma^\mu \tau_R) (\bar{\tau}_R \gamma_\mu \tau_R) + c_{LL}^l (\bar{L}_L \gamma^\mu L_L) (\bar{L}_L \gamma_\mu L_L) \\
& + c_{LR}^{lt} (\bar{L}_L \gamma^\mu L_L) (\bar{t}_R \gamma_\mu t_R) + c_{LR}^{lb} (\bar{L}_L \gamma^\mu L_L) (\bar{b}_R \gamma_\mu b_R) \\
& + c_{LL}^{ql} (\bar{Q}_L \gamma^\mu Q_L) (\bar{L}_L \gamma_\mu L_L) + c_{LL}^{(3)ql} (\bar{Q}_L \gamma^\mu \sigma^a Q_L) (\bar{L}_L \gamma_\mu \sigma^a L_L) + c_{LR}^{q\tau} (\bar{Q}_L \gamma^\mu Q_L) (\bar{\tau}_R \gamma_\mu \tau_R) \\
& + c_{RR}^{t\tau} (\bar{t}_R \gamma^\mu t_R) (\bar{\tau}_R \gamma_\mu \tau_R) + c_{RR}^{b\tau} (\bar{b}_R \gamma^\mu b_R) (\bar{\tau}_R \gamma_\mu \tau_R) \\
& + c_{LR}^b (\bar{Q}_L \gamma^\mu Q_L) (\bar{b}_R \gamma_\mu b_R) + c_{LR}^{(8)b} (\bar{Q}_L \gamma^\mu T^A Q_L) (\bar{b}_R \gamma_\mu T^A b_R) + c_{RR}^b (\bar{b}_R \gamma^\mu b_R) (\bar{b}_R \gamma_\mu b_R) \\
& + c_{RR}^{tb} (\bar{t}_R \gamma^\mu t_R) (\bar{b}_R \gamma_\mu b_R) + c_{RR}^{(8)tb} (\bar{t}_R \gamma^\mu T^A t_R) (\bar{b}_R \gamma_\mu T^A b_R) \\
& + c_{y_t y_\tau} y_t y_\tau (\bar{Q}_L^i t_R) \epsilon_{ij} (\bar{L}_L^j \tau_R) + c'_{y_t y_\tau} y_t y_\tau (\bar{Q}_L^{i\alpha} t_R) \epsilon_{ij} (\bar{L}_L^j t_R^\alpha) + c_{y_\tau y_b} y_\tau y_b^\dagger (\bar{L}_L \tau_R) (\bar{b}_R Q_L) \\
& + c_{y_t y_b} y_t y_b (\bar{Q}_L^i t_R) \epsilon_{ij} (\bar{Q}_L^j b_R) + c_{y_t y_b}^{(8)} y_t y_b (\bar{Q}_L^i T^A t_R) \epsilon_{ij} (\bar{Q}_L^j T^A b_R),
\end{aligned} \tag{A.3}$$

where the last five operators are suppressed in scenarios of minimal flavour violation (MFV), and we have restricted ourselves again to the third generation.

B Electroweak symmetry breaking with dimension-6 operators

Due to the additional terms originating from the dimension-6 operator $\sim |H|^6$, the position of the electroweak minimum changes with respect to the Standard Model prediction. To find the new minimum we consider the potential:

$$V_{SM+6} = \mu^2 |H|^2 + \lambda |H|^4 + \frac{c_6}{\Lambda^2} \lambda |H|^6, \tag{B.1}$$

which contains the additional interaction. Applying the minimisation condition $\partial V / \partial |H|^2 = 0$, we obtain

$$\begin{aligned}
(|H|^2)_\pm &= -\frac{\Lambda^2}{3c_6} \pm \sqrt{\frac{\Lambda^4}{9c_6^2} - \frac{\mu^2 \Lambda^2}{3c_6 \lambda}} \\
&= +\frac{\Lambda^2}{3c_6} \left(-1 \pm \sqrt{1 - \frac{3\mu^2 c_6}{\Lambda^2 \lambda}} \right).
\end{aligned} \tag{B.2}$$

Considering the SM vacuum, i.e. taking the + solution, we obtain :

$$\frac{v^2}{2} \equiv (|H|)_+^2 = \frac{\Lambda^2}{3c_6} \left(-1 + \sqrt{1 - \frac{3\mu^2 c_6}{\Lambda^2 \lambda}} \right), \tag{B.3}$$

which we can solve for μ^2 :

$$\mu^2 = -\lambda v^2 \left(1 + \frac{3}{4} \frac{c_6 v^2}{\Lambda^2} \right). \quad (\text{B.4})$$

Ignoring the Goldstone modes, we can expand the Higgs field $|H|$ in terms of the physical scalar Higgs boson about this minimum, $H \sim (0, (h+v)/\sqrt{2})$. We start by examining the terms arising from the SM Lagrangian and the dimension-6 operators that contribute to the kinetic term:

$$\mathcal{L}_{\text{kin}} = (D_\mu H)^\dagger (D^\mu H) + \frac{c_H}{2\Lambda^2} (\partial^\mu |H|^2)^2, \quad (\text{B.5})$$

where D_μ is the covariant derivative that includes all the interactions of the Higgs field with the gauge bosons. After expansion, we arrive at

$$\begin{aligned} \mathcal{L}_{\text{kin}} &= \frac{1}{2} \left(1 + \frac{c_H v^2}{\Lambda^2} \right) \partial_\mu h \partial^\mu h \\ &+ \frac{c_H v}{\Lambda^2} h \partial_\mu h \partial^\mu h \\ &+ \frac{c_H}{2\Lambda^2} h^2 \partial_\mu h \partial^\mu h + \dots, \end{aligned} \quad (\text{B.6})$$

where we have ignored the gauge boson interactions. To canonically normalise the Higgs boson kinetic term and to remove derivative interactions, we consider the following non-linear transformation:

$$h = \left(1 + \frac{a'_0 v^2}{\Lambda^2} \right) h' + \frac{a'_1 v}{\Lambda^2} h'^2 + \frac{a'_2}{\Lambda^2} h'^3. \quad (\text{B.7})$$

Plugging this into Eq. (B.6), we find the values of the constants a'_i that cancel all terms except $(1/2)\partial_\mu h \partial^\mu h$:

$$a'_0 = -\frac{1}{2} c_H, \quad a'_1 = -\frac{1}{2} c_H, \quad a'_2 = -\frac{1}{6} c_H, \quad (\text{B.8})$$

giving

$$h = \left(1 - \frac{c_H v^2}{2\Lambda^2} \right) h' - \frac{c_H v}{2\Lambda^2} h'^2 - \frac{c_H}{6\Lambda^2} h'^3. \quad (\text{B.9})$$

This shift should be performed *everywhere* in the Lagrangian, and introduces changes in as well as new interactions.

We first perform the shift in the terms contributing to the Higgs boson scalar mass. The relevant terms are:

$$\mathcal{L}_{m_h} = -\frac{\mu^2}{2} h^2 - \frac{3\lambda v^2}{2} h^2 - \frac{15c_6 \lambda v^4}{8\Lambda^2} h^2. \quad (\text{B.10})$$

where the last term comes from the $|H|^6$ interaction. We substitute for μ^2 using Eq. (B.4) and perform the shift of Eq. (B.9), keeping terms up to h^2 and $\mathcal{O}(\Lambda^{-2})$:

$$\begin{aligned} \mathcal{L}_{m_h} &= -\frac{1}{2} \left(2\lambda v^2 + \frac{3c_6 \lambda v^4}{\Lambda^2} \right) \left(1 - \frac{c_H v^2}{2\Lambda^2} \right)^2 h'^2 \\ &= -\lambda v^2 \left(1 + \frac{3c_6 v^2}{2\Lambda^2} - \frac{c_H v^2}{\Lambda^2} \right) h'^2, \end{aligned} \quad (\text{B.11})$$

from which we can immediately deduce the Higgs mass:

$$m_h^2 = 2\lambda v^2 \left(1 - \frac{c_H v^2}{\Lambda^2} + \frac{3c_6 v^2}{2\Lambda^2} \right). \quad (\text{B.12})$$

The terms contributing to multi-Higgs production via gluon fusion at the LHC are:

$$\begin{aligned} \mathcal{L}_{h^n} = & -\mu^2 |H|^2 - \lambda |H|^4 - (y_t \bar{Q}_L H^c t_R + y_b \bar{Q}_L H b_R + \text{h.c.}) \\ & + \frac{c_H}{2\Lambda^2} (\partial^\mu |H|^2)^2 - \frac{c_6}{\Lambda^2} \lambda |H|^6 + \frac{\alpha_s c_g}{4\pi \Lambda^2} |H|^2 G_{\mu\nu}^a G_a^{\mu\nu} \\ & - \left(\frac{c_t}{\Lambda^2} y_t |H|^2 \bar{Q}_L H^c t_R + \frac{c_b}{\Lambda^2} y_b |H|^2 \bar{Q}_L H b_R + \text{h.c.} \right), \end{aligned} \quad (\text{B.13})$$

where we have included in the first line the relevant Standard Model terms that will receive corrections from dimension-6 operators.

We proceed by deriving the expressions for the triple coupling after expanding about the minimum and canonically normalising via Eq. (B.9). The relevant terms are the same as those that appear in the potential of Eq. (B.1):

$$\mathcal{L}_{\text{self}} = -V_{SM+6} = -\mu^2 |H|^2 - \lambda |H|^4 - \frac{c_6}{\Lambda^2} \lambda |H|^6. \quad (\text{B.14})$$

Expanding this about the electroweak minimum, we get

$$\begin{aligned} \mathcal{L}_{\text{self}} = & -\mu^2 \frac{(v+h)^2}{2} - \lambda \frac{(v+h)^4}{4} - \frac{c_6 \lambda (v+h)^6}{\Lambda^2 8} \\ = & -\frac{\mu^2}{2} (v^2 + 2hv + h^2) - \frac{\lambda}{4} (v^4 + 4hv^3 + 6h^2v^2 + 4h^3v + h^4) \\ & - \frac{c_6 \lambda}{8\Lambda^2} (v^6 + 6v^5h + 15v^4h^2 + 20h^3v^3 + 15v^2h^4 + 6h^5v + h^6). \end{aligned} \quad (\text{B.15})$$

Omitting terms with h^n , $n > 4$, and constant terms we arrive at

$$\begin{aligned} \mathcal{L}_{\text{self}} = & -\frac{\mu^2}{2} (2hv + h^2) - \frac{\lambda}{4} (4hv^3 + 6h^2v^2 + 4h^3v + h^4) \\ & - \frac{c_6 \lambda}{8\Lambda^2} (6hv^5 + 15h^2v^4 + 20h^3v^3 + 15h^4v^2) + \dots \end{aligned} \quad (\text{B.16})$$

It is convenient to also calculate the h^2 , h^3 and h^4 terms as a function of h' up to h'^4 :

$$\begin{aligned} h^2 = & h'^2 \left[1 - \frac{c_H v^2}{\Lambda^2} - \frac{c_H v}{\Lambda^2} h' - \frac{c_H}{3\Lambda^2} h'^2 \right] + \mathcal{O}(h'^5), \\ h^3 = & h'^3 \left[1 - \frac{3c_H v^2}{2\Lambda^2} - \frac{3c_H v}{2\Lambda^2} h' \right] + \mathcal{O}(h'^5), \\ h^4 = & h'^4 \left[1 - \frac{2c_H v^2}{\Lambda^2} \right] + \mathcal{O}(h'^5). \end{aligned} \quad (\text{B.17})$$

These terms are then substituted into Eq. (B.16), after which we obtain the terms up to $\mathcal{O}(h'^4)$

$$\begin{aligned} \mathcal{L}_{\text{self}} = & -\lambda \left[v + \frac{5c_6 v^3}{2\Lambda^2} - \frac{5c_H v^3}{2\Lambda^2} \right] h'^3 - \frac{\lambda}{4} \left[1 + \frac{15c_6 v^2}{2\Lambda^2} - \frac{28c_H v^2}{3\Lambda^2} \right] h'^4 + \dots \\ = & -\frac{m_h^2}{2v} \left[1 + \frac{c_6 v^2}{\Lambda^2} - \frac{3c_H v^2}{2\Lambda^2} \right] h'^3 - \frac{m_h^2}{8v^2} \left[1 + \frac{6c_6 v^2}{\Lambda^2} - \frac{25c_H v^2}{3\Lambda^2} \right] h'^4 + \dots \end{aligned} \quad (\text{B.18})$$

Finally, we focus on the fermion-Higgs boson interactions that receive contributions from

$$\mathcal{L}_{hf} = -\frac{y_f}{\sqrt{2}}\bar{f}_L(h+v)f_R - \frac{c_f y_f}{\Lambda^2} \frac{(v+h)^2}{2} \bar{f}_L \frac{(v+h)}{\sqrt{2}} f_R + \text{h.c.}, \quad (\text{B.19})$$

where $f = t, b, \dots$, with $f_{L,R}$ the left- and right-handed fields, and the first term comes from the SM whereas the second term is a dimension-6 contribution. Substituting in the shift of Eq. (B.9), and keeping terms up to $\mathcal{O}(\Lambda^{-2})$, we obtain

$$\begin{aligned} \mathcal{L}_{hf} = & -\frac{y_f v}{\sqrt{2}} \left(1 + \frac{c_t v^2}{2\Lambda^2}\right) \bar{f}_L f_R \\ & -\frac{y_f}{\sqrt{2}} \left(1 - \frac{c_H v^2}{2\Lambda^2} + \frac{3c_f v^2}{2\Lambda^2}\right) \bar{f}_L f_R h' \\ & -\frac{y_f}{\sqrt{2}} \left(\frac{3c_f v}{2\Lambda^2} - \frac{c_H v}{2\Lambda^2}\right) \bar{f}_L f_R h'^2 + \text{h.c.} + \mathcal{O}(h'^3) + \mathcal{O}(\Lambda^{-4}). \end{aligned} \quad (\text{B.20})$$

The first line gives the expression for the modified fermion mass,

$$m_f = \frac{y_f v}{\sqrt{2}} \left(1 + \frac{c_t v^2}{2\Lambda^2}\right), \quad (\text{B.21})$$

and we can re-express Eq. (B.20) in terms of this:

$$\begin{aligned} \mathcal{L}_{hf} = & -m_f \bar{f}_L f_R \\ & -\frac{m_f}{v} \left(1 - \frac{c_H v^2}{2\Lambda^2} + \frac{c_f v^2}{\Lambda^2}\right) \bar{f}_L f_R h' \\ & -\frac{m_f}{v} \left(\frac{3c_f v}{2\Lambda^2} - \frac{c_H v}{2\Lambda^2}\right) \bar{f}_L f_R h'^2 + \text{h.c.} + \mathcal{O}(h'^3) + \mathcal{O}(\Lambda^{-4}). \end{aligned} \quad (\text{B.22})$$

The final term that we need to consider is

$$\begin{aligned} \mathcal{L}_{hg} = & \frac{\alpha_s c_g}{4\pi\Lambda^2} |H|^2 G_{\mu\nu}^a G_a^{\mu\nu} \\ = & \frac{\alpha_s c_g}{4\pi\Lambda^2} \frac{(h+v)^2}{2} G_{\mu\nu}^a G_a^{\mu\nu} \\ = & \frac{\alpha_s c_g}{4\pi\Lambda^2} \left(hv + \frac{h^2}{2}\right) G_{\mu\nu}^a G_a^{\mu\nu} + \dots, \end{aligned} \quad (\text{B.23})$$

where the omitted constant term can be absorbed into an unobservable re-definition of the gluon wave function.

The interactions that contribute to Higgs boson pair production via gluon fusion appear in Eqs. (B.18), (B.22) and (B.23).

References

- [1] **ATLAS** Collaboration, G. Aad et al., *Observation of a new particle in the search for the Standard Model Higgs boson with the ATLAS detector at the LHC*, *Phys.Lett.* **B716** (2012) 1–29, [[arXiv:1207.7214](https://arxiv.org/abs/1207.7214)].

- [2] **CMS Collaboration**, S. Chatrchyan et al., *Observation of a new boson at a mass of 125 GeV with the CMS experiment at the LHC*, *Phys.Lett.* **B716** (2012), no. CMS-HIG-12-028, CERN-PH-EP-2012-220 30–61, [[arXiv:1207.7235](#)].
- [3] F. Englert and R. Brout, *Broken Symmetry and the Mass of Gauge Vector Mesons*, *Phys.Rev.Lett.* **13** (1964) 321–323.
- [4] P. W. Higgs, *Broken Symmetries and the Masses of Gauge Bosons*, *Phys.Rev.Lett.* **13** (1964) 508–509.
- [5] G. Guralnik, C. Hagen, and T. Kibble, *Global Conservation Laws and Massless Particles*, *Phys.Rev.Lett.* **13** (1964) 585–587.
- [6] *CMS-HIG-13-003. CMS-HIG-13-004. CMS-HIG-13-006. CMS-HIG-13-009. CMS-HIG-13-007. CMS-HIG-13-029. CMS-HIG-13-001. CMS-HIG-13-033. CMS-HIG-13-002. CMS-HIG-13-012. CMS-HIG-13-023.*, 2013.
- [7] *ATLAS-CONF-2013-009. ATLAS-CONF-2013-010. ATLAS-CONF-2013-012. ATLAS-CONF-2013-013. ATLAS-HIGG-2013-013. ATLAS-CONF-2014-061. ATLAS-HIGG-2013-23. ATLAS-HIGG-2013-25. ATLAS-HIGG-2013-08. ATLAS-HIGG-2013-21. ATLAS-HIGG-2013-22. ATLAS-HIGG-2013-07.*, 2013, 2014.
- [8] **CMS Collaboration** Collaboration, *Precise determination of the mass of the Higgs boson and studies of the compatibility of its couplings with the standard model*, Tech. Rep. CMS-PAS-HIG-14-009, CERN, Geneva, 2014.
- [9] M. McCullough, *An Indirect Model-Dependent Probe of the Higgs Self-Coupling*, *Phys.Rev.* **D90** (2014), no. 1 015001, [[arXiv:1312.3322](#)].
- [10] T. Plehn and M. Rauch, *The quartic higgs coupling at hadron colliders*, *Phys.Rev.* **D72** (2005) 053008, [[hep-ph/0507321](#)].
- [11] T. Binoth, S. Karg, N. Kauer, and R. Ruckl, *Multi-Higgs boson production in the Standard Model and beyond*, *Phys.Rev.* **D74** (2006) 113008, [[hep-ph/0608057](#)].
- [12] F. Maltoni, E. Vryonidou, and M. Zaro, *Top-quark mass effects in double and triple Higgs production in gluon-gluon fusion at NLO*, *JHEP* **1411** (2014) 079, [[arXiv:1408.6542](#)].
- [13] E. N. Glover and J. van der Bij, *Higgs Boson Pair Production Via Gluon Fusion*, *Nucl.Phys.* **B309** (1988) 282.
- [14] S. Dawson, S. Dittmaier, and M. Spira, *Neutral Higgs boson pair production at hadron colliders: QCD corrections*, *Phys.Rev.* **D58** (1998) 115012, [[hep-ph/9805244](#)].
- [15] A. Djouadi, W. Kilian, M. Muhlleitner, and P. Zerwas, *Production of neutral Higgs boson pairs at LHC*, *Eur.Phys.J.* **C10** (1999) 45–49, [[hep-ph/9904287](#)].
- [16] T. Plehn, M. Spira, and P. Zerwas, *Pair production of neutral Higgs particles in gluon-gluon collisions*, *Nucl.Phys.* **B479** (1996) 46–64, [[hep-ph/9603205](#)].
- [17] D. de Florian and J. Mazzitelli, *Higgs pair production at NNLO*, [[arXiv:1309.6594](#)].
- [18] D. de Florian and J. Mazzitelli, *Two-loop virtual corrections to Higgs pair production*, *Phys.Lett.* **B724** (2013) 306–309, [[arXiv:1305.5206](#)].
- [19] J. Grigo, J. Hoff, K. Melnikov, and M. Steinhauser, *On the Higgs boson pair production at the LHC*, *Nucl.Phys.* **B875** (2013) 1–17, [[arXiv:1305.7340](#)].
- [20] U. Baur, T. Plehn, and D. L. Rainwater, *Determining the Higgs boson selfcoupling at hadron colliders*, *Phys.Rev.* **D67** (2003) 033003, [[hep-ph/0211224](#)].

- [21] U. Baur, T. Plehn, and D. L. Rainwater, *Probing the Higgs selfcoupling at hadron colliders using rare decays*, *Phys.Rev.* **D69** (2004) 053004, [[hep-ph/0310056](#)].
- [22] M. J. Dolan, C. Englert, and M. Spannowsky, *Higgs self-coupling measurements at the LHC*, *JHEP* **1210** (2012) 112, [[arXiv:1206.5001](#)].
- [23] J. Baglio, A. Djouadi, R. Gr uber, M. M ijhleitner, J. Quevillon, et al., *The measurement of the Higgs self-coupling at the LHC: theoretical status*, *JHEP* **1304** (2013) 151, [[arXiv:1212.5581](#)].
- [24] A. J. Barr, M. J. Dolan, C. Englert, and M. Spannowsky, *Di-Higgs final states augmented – selecting hh events at the high luminosity LHC*, *Phys.Lett.* **B728** (2014) 308–313, [[arXiv:1309.6318](#)].
- [25] M. J. Dolan, C. Englert, N. Greiner, and M. Spannowsky, *Further on up the road: hhjj production at the LHC*, *Phys.Rev.Lett.* **112** (2014) 101802, [[arXiv:1310.1084](#)].
- [26] A. Papaefstathiou, L. L. Yang, and J. Zurita, *Higgs boson pair production at the LHC in the $b\bar{b}W^+W^-$ channel*, *Phys.Rev.* **D87** (2013), no. 1 011301, [[arXiv:1209.1489](#)].
- [27] F. Goertz, A. Papaefstathiou, L. L. Yang, and J. Zurita, *Higgs Boson self-coupling measurements using ratios of cross sections*, *JHEP* **1306** (2013) 016, [[arXiv:1301.3492](#)].
- [28] F. Goertz, A. Papaefstathiou, L. L. Yang, and J. Zurita, *Measuring the Higgs boson self-coupling at the LHC using ratios of cross sections*, [arXiv:1309.3805](#).
- [29] P. Maierhoefer and A. Papaefstathiou, *Higgs Boson pair production merged to one jet*, *JHEP* **1403** (2014) 126, [[arXiv:1401.0007](#)].
- [30] C. Englert, F. Krauss, M. Spannowsky, and J. Thompson, *Di-Higgs phenomenology in $t\bar{t}hh$: The forgotten channel*, *Phys.Lett.* **B743** (2015) 93–97, [[arXiv:1409.8074](#)].
- [31] T. Liu and H. Zhang, *Measuring Di-Higgs Physics via the $t\bar{t}hh \rightarrow t\bar{t}b\bar{b}b\bar{b}$ Channel*, [arXiv:1410.1855](#).
- [32] R. Contino, C. Grojean, M. Moretti, F. Piccinini, and R. Rattazzi, *Strong Double Higgs Production at the LHC*, *JHEP* **1005** (2010) 089, [[arXiv:1002.1011](#)].
- [33] M. J. Dolan, C. Englert, and M. Spannowsky, *New Physics in LHC Higgs boson pair production*, *Phys.Rev.* **D87** (2013), no. 5 055002, [[arXiv:1210.8166](#)].
- [34] N. Craig, J. Galloway, and S. Thomas, *Searching for Signs of the Second Higgs Doublet*, [arXiv:1305.2424](#).
- [35] R. S. Gupta, H. Rzehak, and J. D. Wells, *How well do we need to measure the Higgs boson mass and self-coupling?*, *Phys.Rev.* **D88** (2013) 055024, [[arXiv:1305.6397](#)].
- [36] R. Killick, K. Kumar, and H. E. Logan, *Learning what the Higgs boson is mixed with*, *Phys.Rev.* **D88** (2013) 033015, [[arXiv:1305.7236](#)].
- [37] S. Choi, C. Englert, and P. Zerwas, *Multiple Higgs-Portal and Gauge-Kinetic Mixings*, *Eur.Phys.J.* **C73** (2013) 2643, [[arXiv:1308.5784](#)].
- [38] J. Cao, Z. Heng, L. Shang, P. Wan, and J. M. Yang, *Pair Production of a 125 GeV Higgs Boson in MSSM and NMSSM at the LHC*, *JHEP* **1304** (2013) 134, [[arXiv:1301.6437](#)].
- [39] D. T. Nhung, M. Muhlleitner, J. Streicher, and K. Walz, *Higher Order Corrections to the Trilinear Higgs Self-Couplings in the Real NMSSM*, *JHEP* **1311** (2013) 181, [[arXiv:1306.3926](#)].

- [40] J. Galloway, M. A. Luty, Y. Tsai, and Y. Zhao, *Induced Electroweak Symmetry Breaking and Supersymmetric Naturalness*, *Phys.Rev.* **D89** (2014) 075003, [[arXiv:1306.6354](#)].
- [41] U. Ellwanger, *Higgs pair production in the NMSSM at the LHC*, *JHEP* **1308** (2013) 077, [[arXiv:1306.5541](#)].
- [42] C. Han, X. Ji, L. Wu, P. Wu, and J. M. Yang, *Higgs pair production with SUSY QCD correction: revisited under current experimental constraints*, *JHEP* **1404** (2014) 003, [[arXiv:1307.3790](#)].
- [43] J. M. No and M. Ramsey-Musolf, *Probing the Higgs Portal at the LHC Through Resonant di-Higgs Production*, *Phys.Rev.* **D89** (2014), no. 9 095031, [[arXiv:1310.6035](#)].
- [44] R. Grober and M. Muhlleitner, *Composite Higgs Boson Pair Production at the LHC*, *JHEP* **1106** (2011) 020, [[arXiv:1012.1562](#)].
- [45] R. Contino, M. Ghezzi, M. Moretti, G. Panico, F. Piccinini, et al., *Anomalous Couplings in Double Higgs Production*, *JHEP* **1208** (2012) 154, [[arXiv:1205.5444](#)].
- [46] M. Gillioz, R. Grober, C. Grojean, M. Muhlleitner, and E. Salvioni, *Higgs Low-Energy Theorem (and its corrections) in Composite Models*, *JHEP* **1210** (2012) 004, [[arXiv:1206.7120](#)].
- [47] G. D. Kribs and A. Martin, *Enhanced di-Higgs Production through Light Colored Scalars*, *Phys.Rev.* **D86** (2012) 095023, [[arXiv:1207.4496](#)].
- [48] S. Dawson, E. Furlan, and I. Lewis, *Unravelling an extended quark sector through multiple Higgs production?*, *Phys.Rev.* **D87** (2013) 014007, [[arXiv:1210.6663](#)].
- [49] C.-Y. Chen, S. Dawson, and I. Lewis, *Top Partners and Higgs Boson Production*, *Phys.Rev.* **D90** (2014), no. 3 035016, [[arXiv:1406.3349](#)].
- [50] K. Nishiwaki, S. Niyogi, and A. Shivaji, *ttH Anomalous Coupling in Double Higgs Production*, *JHEP* **1404** (2014) 011, [[arXiv:1309.6907](#)].
- [51] J. Liu, X.-P. Wang, and S.-h. Zhu, *Discovering extra Higgs boson via pair production of the SM-like Higgs bosons*, [arXiv:1310.3634](#).
- [52] T. Enkhbat, *Scalar leptoquarks and Higgs pair production at the LHC*, *JHEP* **1401** (2014) 158, [[arXiv:1311.4445](#)].
- [53] Z. Heng, L. Shang, Y. Zhang, and J. Zhu, *Pair production of 125 GeV Higgs boson in the SM extension with color-octet scalars at the LHC*, *JHEP* **1402** (2014) 083, [[arXiv:1312.4260](#)].
- [54] R. Frederix, S. Frixione, V. Hirschi, F. Maltoni, O. Mattelaer, et al., *Higgs pair production at the LHC with NLO and parton-shower effects*, *Phys.Lett.* **B732** (2014) 142–149, [[arXiv:1401.7340](#)].
- [55] J. Baglio, O. Eberhardt, U. Nierste, and M. Wiebusch, *Benchmarks for Higgs Pair Production and Heavy Higgs Searches in the Two-Higgs-Doublet Model of Type II*, *Phys.Rev.* **D90** (2014) 015008, [[arXiv:1403.1264](#)].
- [56] B. Hespel, D. Lopez-Val, and E. Vryonidou, *Higgs pair production via gluon fusion in the Two-Higgs-Doublet Model*, *JHEP* **1409** (2014) 124, [[arXiv:1407.0281](#)].
- [57] B. Bhattacharjee and A. Choudhury, *The role of MSSM heavy Higgs production in the self coupling measurement of 125 GeV Higgs boson at the LHC*, [arXiv:1407.6866](#).

- [58] N. Liu, S. Hu, B. Yang, and J. Han, *Impact of top-Higgs couplings on Di-Higgs production at future colliders*, *JHEP* **1501** (2015) 008, [[arXiv:1408.4191](#)].
- [59] J. Cao, D. Li, L. Shang, P. Wu, and Y. Zhang, *Exploring the Higgs Sector of a Most Natural NMSSM and its Prediction on Higgs Pair Production at the LHC*, *JHEP* **1412** (2014) 026, [[arXiv:1409.8431](#)].
- [60] B. Grinstein and M. Trott, *A Higgs-Higgs bound state due to new physics at a TeV*, *Phys.Rev.* **D76** (2007) 073002, [[arXiv:0704.1505](#)].
- [61] R. Alonso, M. Gavela, L. Merlo, S. Rigolin, and J. Yepes, *The Effective Chiral Lagrangian for a Light Dynamical "Higgs Particle"*, *Phys.Lett.* **B722** (2013) 330–335, [[arXiv:1212.3305](#)].
- [62] G. Buchalla, O. Catà, and C. Krause, *Complete Electroweak Chiral Lagrangian with a Light Higgs at NLO*, *Nucl.Phys.* **B880** (2014) 552–573, [[arXiv:1307.5017](#)].
- [63] W. Buchmuller and D. Wyler, *Effective Lagrangian Analysis of New Interactions and Flavor Conservation*, *Nucl.Phys.* **B268** (1986) 621–653.
- [64] B. Grzadkowski, M. Iskrzynski, M. Misiak, and J. Rosiek, *Dimension-Six Terms in the Standard Model Lagrangian*, *JHEP* **1010** (2010) 085, [[arXiv:1008.4884](#)].
- [65] J. Elias-Miro, J. Espinosa, E. Masso, and A. Pomarol, *Higgs windows to new physics through $d=6$ operators: constraints and one-loop anomalous dimensions*, *JHEP* **1311** (2013) 066, [[arXiv:1308.1879](#)].
- [66] A. Pomarol and F. Riva, *Towards the Ultimate SM Fit to Close in on Higgs Physics*, *JHEP* **1401** (2014) 151, [[arXiv:1308.2803](#)].
- [67] B. Dumont, S. Fichet, and G. von Gersdorff, *A Bayesian view of the Higgs sector with higher dimensional operators*, *JHEP* **1307** (2013) 065, [[arXiv:1304.3369](#)].
- [68] T. Corbett, O. Eboli, J. Gonzalez-Fraile, and M. Gonzalez-Garcia, *Constraining anomalous Higgs interactions*, *Phys.Rev.* **D86** (2012) 075013, [[arXiv:1207.1344](#)].
- [69] T. Corbett, O. Eboli, J. Gonzalez-Fraile, and M. Gonzalez-Garcia, *Robust Determination of the Higgs Couplings: Power to the Data*, *Phys.Rev.* **D87** (2013) 015022, [[arXiv:1211.4580](#)].
- [70] T. Corbett, O. Eboli, J. Gonzalez-Fraile, and M. Gonzalez-Garcia, *Determining Triple Gauge Boson Couplings from Higgs Data*, *Phys.Rev.Lett.* **111** (2013), no. 1 011801, [[arXiv:1304.1151](#)].
- [71] R. Contino, M. Ghezzi, C. Grojean, M. Muhlleitner, and M. Spira, *Effective Lagrangian for a light Higgs-like scalar*, *JHEP* **1307** (2013) 035, [[arXiv:1303.3876](#)].
- [72] M. Trott, *On the consistent use of Constructed Observables*, *JHEP* **1502** (2015) 046, [[arXiv:1409.7605](#)].
- [73] G. Giudice, C. Grojean, A. Pomarol, and R. Rattazzi, *The Strongly-Interacting Light Higgs*, *JHEP* **0706** (2007) 045, [[hep-ph/0703164](#)].
- [74] G. D’Ambrosio, G. Giudice, G. Isidori, and A. Strumia, *Minimal flavor violation: An Effective field theory approach*, *Nucl.Phys.* **B645** (2002) 155–187, [[hep-ph/0207036](#)].
- [75] F. Goertz, *Indirect Handle on the Down-Quark Yukawa Coupling*, *Phys.Rev.Lett.* **113** (2014), no. 26 261803, [[arXiv:1406.0102](#)].
- [76] C. Arzt, M. Einhorn, and J. Wudka, *Patterns of deviation from the standard model*, *Nucl.Phys.* **B433** (1995) 41–66, [[hep-ph/9405214](#)].

- [77] M. B. Einhorn and J. Wudka, *The Bases of Effective Field Theories*, *Nucl.Phys.* **B876** (2013) 556–574, [[arXiv:1307.0478](#)].
- [78] E. E. Jenkins, A. V. Manohar, and M. Trott, *On Gauge Invariance and Minimal Coupling*, *JHEP* **1309** (2013) 063, [[arXiv:1305.0017](#)].
- [79] T. Plehn, *Lectures on LHC Physics*, *Lect.Notes Phys.* **844** (2012) 1–193, [[arXiv:0910.4182](#)].
- [80] Wolfram Research Inc., *Mathematica*, 2014.
- [81] N. D. Christensen and C. Duhr, *FeynRules - Feynman rules made easy*, *Comput.Phys.Commun.* **180** (2009) 1614–1641, [[arXiv:0806.4194](#)].
- [82] A. Alloul, N. D. Christensen, C. Degrande, C. Duhr, and B. Fuks, *FeynRules 2.0 - A complete toolbox for tree-level phenomenology*, *Comput.Phys.Commun.* **185** (2014) 2250–2300, [[arXiv:1310.1921](#)].
- [83] M. Farina, C. Grojean, F. Maltoni, E. Salvioni, and A. Thamm, *Lifting degeneracies in Higgs couplings using single top production in association with a Higgs boson*, *JHEP* **1305** (2013) 022, [[arXiv:1211.3736](#)].
- [84] R. Contino, M. Ghezzi, C. Grojean, M. Majhlleitner, and M. Spira, *eHDECAY: an Implementation of the Higgs Effective Lagrangian into HDECAY*, *Comput.Phys.Commun.* **185** (2014) 3412–3423, [[arXiv:1403.3381](#)].
- [85] “hpair program.” <http://people.web.psi.ch/spira/hpair/>.
- [86] F. Goertz, A. Papaefstathiou, L. L. Yang, and J. Zurita, *Improved analysis of Higgs boson pair production in the D=6 extension of the SM*, .
- [87] C. Englert and M. Spannowsky, *Effective Theories and Measurements at Colliders*, [arXiv:1408.5147](#).
- [88] A. Martin, W. Stirling, R. Thorne, and G. Watt, *Parton distributions for the LHC*, *Eur.Phys.J.* **C63** (2009) 189–285, [[arXiv:0901.0002](#)].
- [89] S. Frixione, F. Stoeckli, P. Torrielli, and B. R. Webber, *NLO QCD corrections in Herwig++ with MC@NLO*, *JHEP* **1101** (2011) 053, [[arXiv:1010.0568](#)].
- [90] R. Frederix, S. Frixione, V. Hirschi, F. Maltoni, R. Pittau, et al., *Scalar and pseudoscalar Higgs production in association with a top-antitop pair*, *Phys.Lett.* **B701** (2011) 427–433, [[arXiv:1104.5613](#)].
- [91] J. Alwall, R. Frederix, S. Frixione, V. Hirschi, F. Maltoni, et al., *The automated computation of tree-level and next-to-leading order differential cross sections, and their matching to parton shower simulations*, *JHEP* **1407** (2014) 079, [[arXiv:1405.0301](#)].
- [92] V. Ahrens, A. Ferroglia, M. Neubert, B. D. Pecjak, and L. L. Yang, *Precision predictions for the $t\bar{t}$ production cross section at hadron colliders*, *Phys.Lett.* **B703** (2011) 135–141, [[arXiv:1105.5824](#)].
- [93] M. Czakon, P. Fiedler, and A. Mitov, *The total top quark pair production cross-section at hadron colliders through $O(\alpha_S^4)$* , *Phys.Rev.Lett.* **110** (2013) 252004, [[arXiv:1303.6254](#)].
- [94] M. Bahr, S. Gieseke, and M. H. Seymour, *Simulation of multiple partonic interactions in Herwig++*, *JHEP* **0807** (2008) 076, [[arXiv:0803.3633](#)].
- [95] M. Cacciari, G. P. Salam, and G. Soyez, *FastJet User Manual*, *Eur.Phys.J.* **C72** (2012) 1896, [[arXiv:1111.6097](#)].

- [96] M. Cacciari and G. P. Salam, *Dispelling the N^3 myth for the k_t jet-finder*, *Phys.Lett.* **B641** (2006) 57–61, [[hep-ph/0512210](#)].
- [97] J. M. Butterworth, A. R. Davison, M. Rubin, and G. P. Salam, *Jet substructure as a new Higgs search channel at the LHC*, *Phys.Rev.Lett.* **100** (2008) 242001, [[arXiv:0802.2470](#)].
- [98] P. Bechtle, O. Brein, S. Heinemeyer, O. Stål, T. Stefaniak, et al., *HiggsBounds – 4: Improved Tests of Extended Higgs Sectors against Exclusion Bounds from LEP, the Tevatron and the LHC*, *Eur.Phys.J.* **C74** (2014) 2693, [[arXiv:1311.0055](#)].
- [99] P. Bechtle, S. Heinemeyer, O. Stål, T. Stefaniak, and G. Weiglein, *HiggsSignals: Confronting arbitrary Higgs sectors with measurements at the Tevatron and the LHC*, *Eur.Phys.J.* **C74** (2014) 2711, [[arXiv:1305.1933](#)].
- [100] B. A. Kniehl and M. Spira, *Low-energy theorems in Higgs physics*, *Z.Phys.* **C69** (1995) 77–88, [[hep-ph/9505225](#)].
- [101] A. Freitas and P. Schwaller, *Higgs CP Properties From Early LHC Data*, *Phys.Rev.* **D87** (2013), no. 5 055014, [[arXiv:1211.1980](#)].
- [102] J. Brod, U. Haisch, and J. Zupan, *Constraints on CP-violating Higgs couplings to the third generation*, *JHEP* **1311** (2013) 180, [[arXiv:1310.1385](#)].
- [103] M. J. Dolan, P. Harris, M. Jankowiak, and M. Spannowsky, *Constraining CP-violating Higgs Sectors at the LHC using gluon fusion*, *Phys.Rev.* **D90** (2014), no. 7 073008, [[arXiv:1406.3322](#)].